Journal of Neuroscience Research 38:327–335 (1994)

Lesion-Specific Pattern of Immunocytochemical Distribution of Growth-Associated Protein B-50 (GAP-43) in the Cerebellum of Weaver and PCD-Mutant Mice: Lack of B-50 Involvement in Neuroplasticity of Purkinje Cell Terminals?

J. Bäurle, A.B. Oestreicher, W.H. Gispen, and U. Grüsser-Cornehls
Department of Physiology, Freie Universität Berlin, Berlin, Germany (J.B., U.G.-C.); Division of Molecular Neurobiology, Rudolf Magnus Institute and Institute of Molecular Biology and Medical Biotechnology, University of Utrecht, Utrecht, The Netherlands (A.B.O., W.H.G.)

The growth-associated protein B-50 (GAP-43) is thought to play a major role in the development and regeneration of neurons. The participation of B-50 in neuronal plasticity is well documented, especially for monoaminergic systems. However, such an important role for B-50 in GABAergic systems has not been substantiated to date. This study was performed to obtain detailed information about the identity of B-50 immunopositive axons and terminals in the cerebellum and to test the involvement of this protein during plastic changes as observed in the projections of GABAergic Purkinje cells to the lateral vestibular nucleus (LVN). For this purpose mutant mice with specific cerebellar cell loss were used. Weaver mutants (B6CBA *wv*/*wv*), PCD-mutants (B6C3Fe *pcd*/*pcd*), and their corresponding wild-type mice were investigated with immunocytochemical and immunoblot procedures at the age of 8–23 days and 5–6 months using polyclonal and monoclonal antibodies to B-50. Substantial differences in B-50 distribution were detected between normals and mutants and between young and adult animals. These results demonstrate that the labeling of B-50 is mainly related to the outgrowth of parallel fibers and to a minor degree on the ingrowth of non-GABAergic cerebellar afferents. There was no immunocytochemical indication that B-50 is related to Purkinje cells or accompanies the plasticity of the GABAergic innervation of the LVN. © 1994 Wiley-Liss, Inc.

Key words: B-50 (GAP-43), plasticity, GABAergic, Weaver mutant, PCD-mutant, parallel fibers, Purkinje cells, lateral vestibular nucleus

INTRODUCTION

The phosphoprotein B-50 (Zwiers et al., 1980), also known as GAP-43 (Jacobson et al., 1986), F1 (Akers and Routtenberg, 1985), pp46 (Katz et al., 1985), or p57 (neuromodulin) (Andreasen et al., 1983), a rapidly transported (Skene and Willard, 1981) substrate of the protein kinase C (Aloyo et al., 1983), is found to be synthesized by neurons during normal central nervous system (CNS) development (Jacobson et al., 1986). As they mature, elevated levels of this protein only remain in special subsets of neurons, some of them being characterized by the continued potency of synaptic plasticity, while others are not (Skene, 1989).

In addition, injury to neurons, in particular to their axons, can lead to a reinduction of a high B-50 expression in neurons of the adult peripheral nervous system (PNS) and in nerve cells of the CNS capable of sprouting (Skene, 1989). Consequently, B-50 is thought to be a candidate for assisting neurons in their ability to grow axons or axon collaterals or to maintain the capacity of synaptic remodeling during a lifetime (Benowitz and Routtenberg, 1987; Neve et al., 1988; Benowitz et al., 1990). This is relatively well documented in monoaminergic systems (Bendotti et al., 1991), but evidence is lacking so far in brain areas where the density of GABAergic neurons is high.

A system in which GABA is a very predominant

Received March 22, 1993; revised November 9, 1993; accepted November 18, 1993.

Address reprint requests to J. Bäurle, Department of Physiology, Freie Universität Berlin, Arnimallee 22, 14195 Berlin, Germany.

transmitter is the cerebellum and its projection areas, the deep cerebellar nuclei and the vestibular nuclei. In intact neurons, neuronal somata are virtually unstained by B-50 immunocytochemistry (Oestreicher and Gispen, 1986; Mercken et al., 1992) and therefore it is not yet fully clarified to which neurons of the cerebellar cortex and the terminal domains of the cerebellum the recently described positivity of fibers and terminals is related (Oestreicher and Gispen, 1986). The existence of cerebellar-affected mouse mutants with specific cell degeneration makes them natural subjects for revealing the influence of cell loss on the distribution of B-50 (GAP-43) in the cerebellum and its projection areas and gaining more insight into the identity of B-50 positive elements under normal conditions. Two of these mutants, the Weaver mutant and the PCD-mutant, were chosen for the present study. In Weaver mutants a rapid and almost total loss of granule cells occurs in the first 3 postnatal weeks (P0–P20) (Smeyne and Goldowitz, 1989): only a few granule cells survive in the hemispheres, whereas vermal and intermediate regions are virtually agranular in adult animals (Rakic and Sidman, 1973a,b). Furthermore, a less pronounced Purkinje cell degeneration in Weaver with an overall loss of 25% of Purkinje cells, but to a higher extent in the Vermis (up to 50%), is reported (Blatt and Eisenman, 1985). In PCD-mutants the gene defect leads to a postnatal degeneration of more than 99% of all Purkinje cells by the fourth postnatal week (Mullen et al., 1976; Wassef et al., 1986). The severity of cell damage in both mutants makes them particularly suited for this kind of study. Moreover, as described in a recent study (Bäurle and Grüsser-Cornehls, 1992; Bäurle et al., 1992), a continuous remodeling of synaptic terminals in normal wild types and terminal expansion and collateral sprouting in Weaver mutants are present in the dorsal part of the lateral vestibular nucleus (LVN), which receives a massive GABAergic input of Purkinje cells, mainly of vermal origin (Brodal, 1981). Therefore, this area is interesting to test for B-50 participation in the plasticity of a GABAergic system.

To our knowledge this is the first report on the distribution of B-50 in the cerebella of mutant mice.

MATERIALS AND METHODS

For comparative immunocytochemical and immunoblot investigations 29 mice were used, the parents of which were derived originally from Jackson Laboratories (Bar Harbor, ME); the offspring were maintained at the Department of Physiology, Freie Universität Berlin, on a natural dark/light rhythm and food and water ad libitum: 12 Weaver mutants (B6CBA *wv/wv*) (6 at 8–23 days and 6 at 5–6 months of age), 9 B6CBA-wild types (+/+) (5/4), 4 PCD-mutants (B6C3Fe *pcd/pcd*) (1/3), and 4 C57BL6J-wild types (+/+) (2/2). Young and adult animals were chosen to test for differences between postnatal development and maturity.

Immunocytochemistry

Immunocytochemistry was performed according to the peroxidase-antiperoxidase (PAP) method (Sternberger et al., 1970). The B-50 antibody used was a polyclonal affinity-purified rabbit (8920/8921) antibody raised against B-50 purified from adult rat brain and has been characterized by Oestreicher et al. (1983) and Oestreicher and Gispen (1986). All incubation steps of sections from age-matched animals were performed simultaneously in the same solutions. Perfusion started with normal saline (0.9%) in 0.067 M PO_4 buffer at pH 7.4 under deep chloral-hydrate anesthesia (1.75 g/kg body weight) and was followed by the fixative containing 2% paraformaldehyde (Merck, Darmstadt, Germany) and 0.5% glutaraldehyde (Merck) in 0.1 M PO_4 buffer at pH 7.4 for 15 min. After 2 hr of postfixation in the same fixative, brains were cut in the coronal plane at 30 μm on a vibratome (TPI Series 1000, Technical Products International, St. Louis, MO). Sections were treated first with 10% methanol and 3% H_2O_2 in 0.01 M phosphate buffered saline (PBS) at pH 7.5 in order to block endogenous peroxidase activity. This was followed by washing twice in distilled water for 5 min and subsequent washing in Tris buffered saline (TBS) consisting of 0.05 M Tris-HCl, pH 7.6, and 0.9% NaCl. To prevent nonspecific binding of the first antibody, preincubation with a solution containing normal goat serum (NGS) (Dako, Hamburg, Germany) at 10%, bovine serum albumin (BSA) at 0.1%, and Triton X-100 (Sigma, Munchen, Germany) at 1% in TBS was performed. In preliminary tests various dilutions of the first antibody (anti-B-50 immunoglobulins) were screened to obtain optimal immunostaining; intense staining in the cerebellar molecular layer of neonatal animals was assessed as being suitable (Oestreicher and Gispen, 1986), so that a dilution of 1:600 of the B-50 antibody in TBS containing 5% NGS and 0.3% Triton X-100 was selected. The first antibody incubation was performed at 4°C for 16 hr in a humid chamber under gentle agitation. Control sections were incubated in the same solution with NGS added but without the first antibody. Three washes in TBS followed prior to incubation with the second antibody, goat-anti-rabbit (Dako) 1:150, diluted in the same solution as the primary antibody. 1) Washing 3 × 5 min in TBS. Sections were then incubated in the PAP-complex (Dako) 1:50. 2) Washing 3 × 5 min in TBS. The presence of the peroxidase enzyme was revealed by 0.05% diaminobenzidine (DAB) (Sigma) in TBS containing 1% H_2O_2 for 15 min. 3) Finally sections were washed in TBS and deionized water and then mounted, dehydrated, and coverslipped

as usual. In some cases sections were Nissl-counterstained for better identification of cell bodies and nuclear borders.

Immunoblots

Ten percent (w/v) homogenates of mouse brain tissue in 0.5% Triton X-100, 0.1 mM EGTA, 1 mM NaF in PBS (10 mM phosphate buffer, 0.150 M NaCl at pH 7.4) were prepared. In order to prevent proteolysis the homogenation mix contained 2 mM PMSF and 0.3 μM Trasylol. Protein content of the homogenates was determined with the Pierce (Rockville, IL) protein kit.

Samples containing either 50, 25, or 10 μg protein of the brain homogenates were solubilized in hot solubilization mix [containing in final concentrations: 2% sodium dodecyl sulfate (SDS), 5% β-mercaptoethanol, 10% glycerol, and 68 mM Tris-HCl at pH 6.8]. Samples were loaded on a 11% polyacrylamide gel containing SDS and electrophoresed. The gel containing resolved proteins was immediately electroblotted onto nitrocellulose (Schleicher & Schuell, Kassel, Germany) according to the procedure described by Towbin et al. (1979). Western blots were inactivated by a solution containing 10% dried skimmed milk powder in PBS for 30 min at room temperature. Thereafter, blots were immunoreacted with the primary antibody: 1:1,000 diluted polyclonal affinity-purified antibodies (of rabbit 8920/8921 raised against rat B-50) or 1:4,000 diluted monoclonal mouse B-50 antibodies (NM4). The characterization of these B-50 antibodies has been described by Oestreicher et al. (1983) and Mercken et al. (1992). After thorough rinsing, the blots were incubated with goat-anti-rabbit antibodies conjugated to alkaline phosphatase (Promega, Madison, WI) or with goat-anti-mouse antibodies conjugated to alkaline phosphatase (Jackson Immunoresearch, West Grove, PA). Finally, after removing excess second antibody by repeated rinsing, the immunoreaction was visualized by the enzyme-substrate reaction of (0.15 mg/ml) nitroblue tetrazolium salt (Sigma) and (0.075 mg/ml) 5-bromo-4-chloro-3-indolyl phosphate (Sigma) in 0.1 M Tris-HCl, 0.1 M NaCl, 5 mM MgCl at pH 9.5.

RESULTS

Immunocytochemistry

Wild types. The distribution of B-50 in the cerebellum of normal mice revealed by the present investigation is in general agreement with that described in the rat (Oestreicher and Gispen, 1986). In wild types (B6CBA as well as B6C3Fe) at an age of 8–10 days (see Figs. 1, 2) immunolabeling in the cerebellar cortex is attributed mainly to the premigratory zone (pmz) of the external granular layer (egl) and to the molecular layer (ML). The superficial part of the egl is completely devoid of staining. In the internal granular layer (igl) only weak staining is present. Purkinje cells are immunonegative but surrounded by positive dots and fibers (for higher magnification, see Fig. 3B). In the white matter a substantial number of heavily labeled fibers is visible. The deep nuclei (DCN) and the LVN are almost devoid of staining (see Fig. 1). Figure 3A presents a higher power photograph of the pmz, which is characterized at this age by heavily immunostained processes extending from the the egl into the upper part of the ML.

With the exception of the egl, which is no longer present, the same pattern of immunolabeling is found in 23-day-old and 5–6-month-old animals but at an overall weaker level. The intensity of staining in the 3-week-old animals (not shown) already closely resembles the low B-50 level in 5-month-old animals (see Figs. 1, 2). The most drastic decrease in comparison to the immature cerebellum occurs in the white matter and the igl. The labeling intensity of dots and fibers surrounding the Purkinje cell somata also decreases in the mature cerebellum. The target nuclei of cerebellar projections (DCN and dorsal part of the LVN) are again almost immunonegative. Interestingly, positive fibers in the inferior cerebellar peduncle (icp) appear *only* in the adult animals (see Fig. 1B).

Mutants. Due to the granule cell deficit and the ectopic localization of Purkinje cells in the Weaver mutant, the obvious layering of the cerebellar cortex, as seen in wild types, is lost (Sotelo, 1982). The pattern of B-50 immunolabeling is therefore quite different from that seen in wild types (see Figs. 1, 2). In the 10-day-old mutant the whole egl, including the pmz, is almost devoid of staining, while the presumptive molecular layer (pml) exhibits a weak staining intensity, which is related mainly to immunopositive dots surrounding the Purkinje cells scattered ectopically in this pml. The immunopositive processes, shown in Figure 3A for the wild type, are completely missing (see Fig. 2B). The only consistent labeling in the young Weaver mutant is found in fibers traversing the white matter (see Fig. 2). Staining intensity in the terminal domains of the GABAergic Purkinje cells (DCN and vestibular nuclei) is again only at a background level (see Fig. 1).

In adult Weaver mutants the intensity of staining in the cerebellum declines to almost unrecognizable levels, except for the white matter, where some very moderately labeled fibers remain (see Fig. 2). Also the deep cerebellar nuclei and the LVN are completely devoid of staining.

To exclude the possibility that the scarce distribution of B-50 in the Weaver cerebellum is caused to some extent by the partial loss of Purkinje cells, PCD-mutants were tested in addition. As seen in Figure 4, the distribution of B-50 in these PCD-mutants closely resembles that seen in normal wild types (see Fig. 2C for comparison), with the one exception that immunoreactive dots

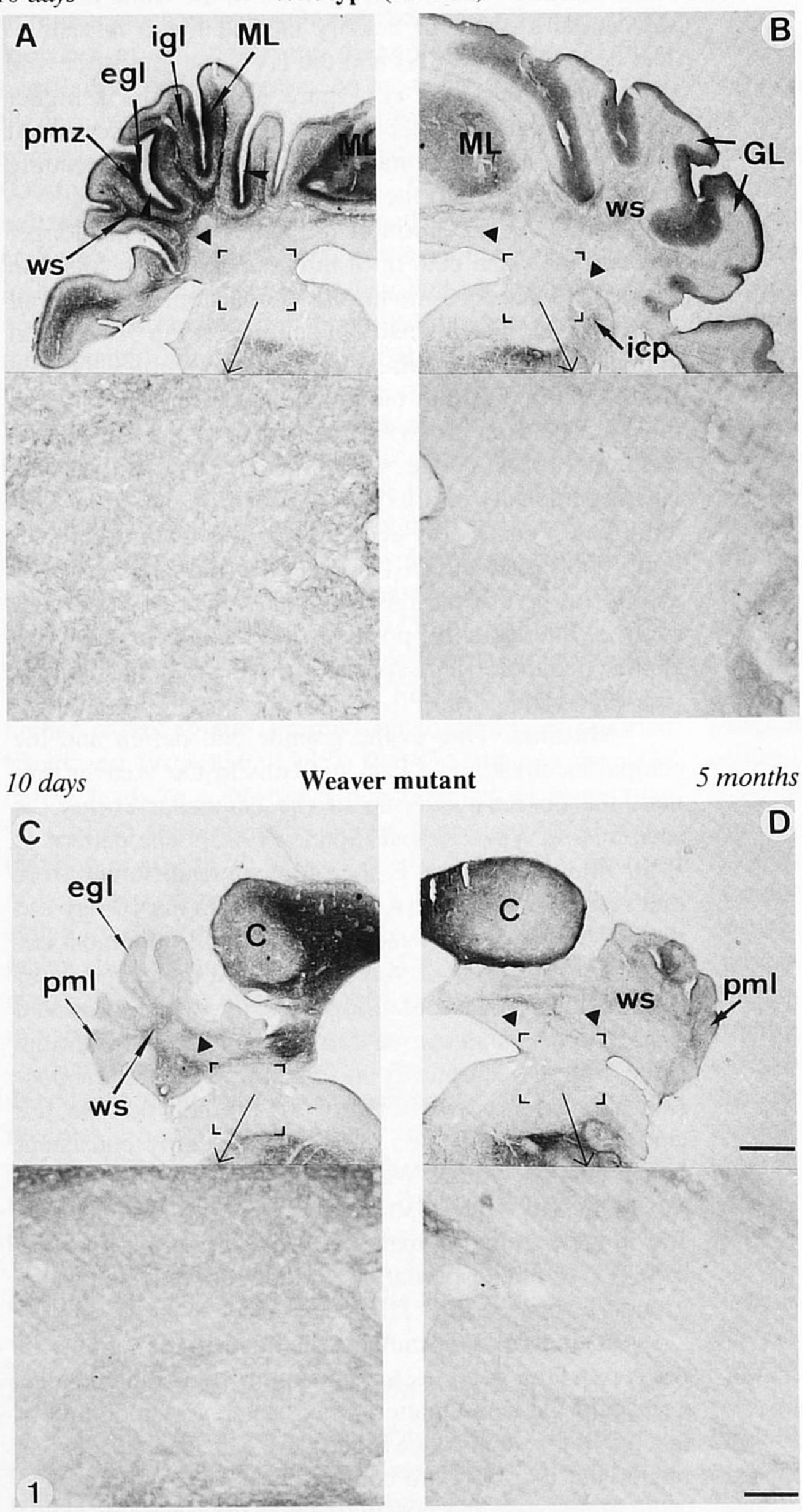

Fig. 1. B-50 immunoreactivity in the cerebellar cortex and brainstem of immature and adult wild types (**A,B**) and Weaver mutants (**C,D**). The rostrocaudal level of the sections is at the deep cerebellar nuclei and the vestibular nuclei. Each hemisection is provided with an inlay, which shows the area that includes the dorsal part of the LVN, in which sprouting and remodeling of GABAergic terminals occur. **A:** Ten-day-old wild type; the highest density of the immunoreaction product is visible in the premigratory zone (pmz) of the external granule layer (egl) and in the molecular layer (ML), the superficial part of the egl (arrowheads) is completely immunonegative. In the white substance (ws), densely labeled fibers are visible, whereas the internal granule cell layer (igl) is only weakly labeled. The deep nuclei (triangle) and the dorsal part of the LVN (see **inlay**) remain almost unstained. **B:** Five-month-old wild type; an overall decrease in the intensity of the B-50 immunolabeling compared to the immature state is obvious. Consistent B-50 immunoreactivity is only detectable in the ML. Some moderately stained fibers are visible in the ws. The terminal domains of the cerebellum (DCN and LVN: see triangles and **inlay**) are completely unstained, whereas some fibers in the inferior cerebellar peduncle (icp) are immunopositive. GL = granule cell layer. **C:** Ten-day-old Weaver mutant; B-50 is present in fibers traversing the ws but absent in the egl and very thinly distributed in the presumptive molecular layer (pml). Deep nuclei (triangle) and dorsal part of the LVN (see **inlay**) are again almost unlabeled. C = superior colliculus. **D:** Five-month-old Weaver mutant; immunolabeling is no longer detectable at this magnification, neither in the cerebellum nor in the terminal domains of the cerebellum. × 13.8. Bar = 640 μm. Inlays: × 62.4. Bar = 100 μm.

and fibers surrounding the Purkinje cell somata are missing in young and adult PCD-mutants (data not shown).

Immunoblots

In all mouse samples and with both poly- and monoclonal antibodies, B-50 is detected at the same position as the reference B-50 in rat brain (see Fig. 5). Similar results were obtained with similar samples of hemispheres and cerebellum derived from the B6C3Fe-wild types (14 days old or 5 months old), the PCD-mutants (4–5 months old), and the B6CBA-wild type (12 days old). This clearly demonstrates the presence of

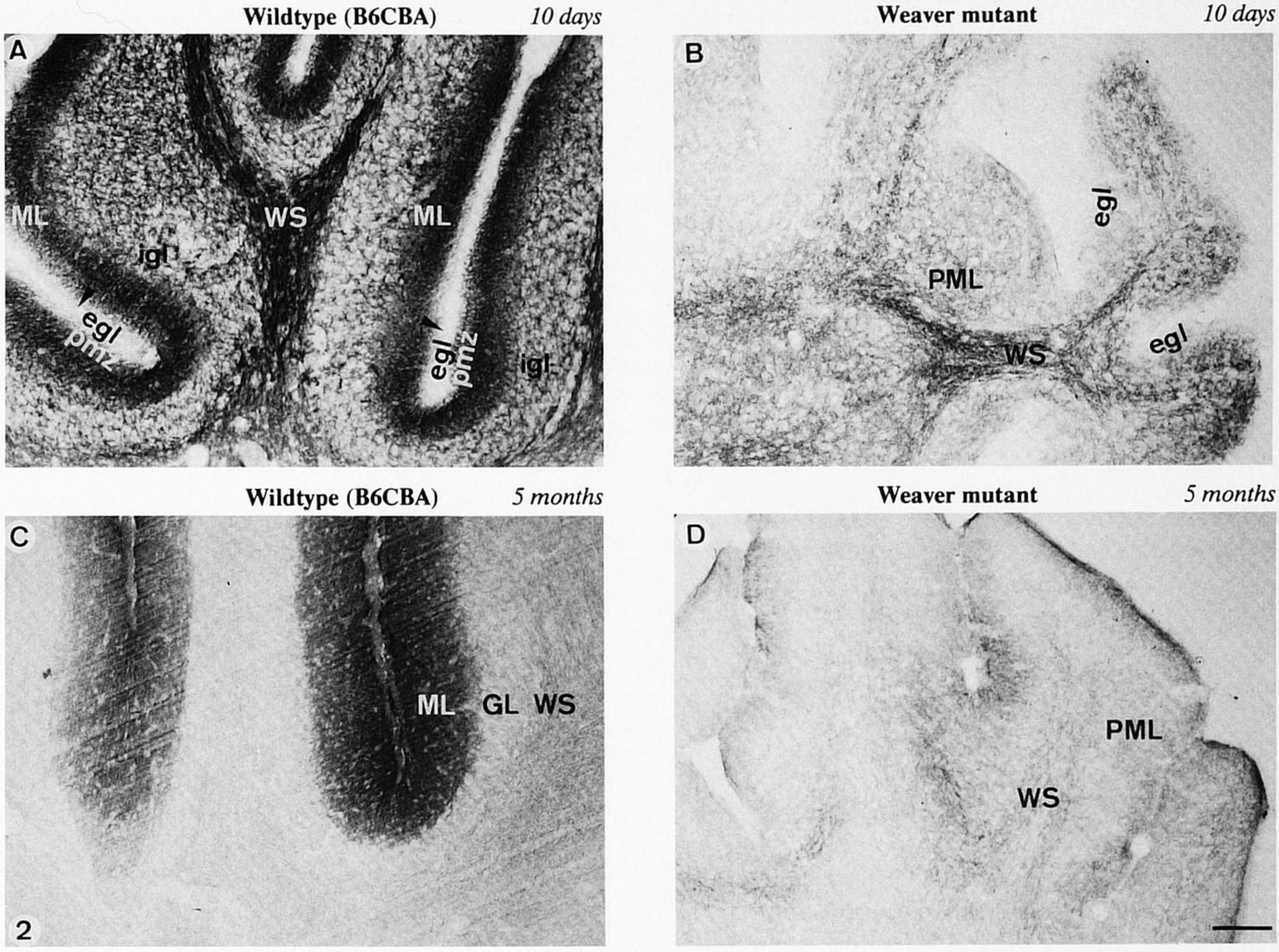

Fig. 2. B-50 immunostained cerebellar cortex of wild types (**A,C**) and Weaver mutants (**B,D**). **A,B:** Ten-day-old wild type and age-matched Weaver mutant show drastic differences in the B-50 staining pattern: in the wild type only the superficial part of the external granule layer (egl) (arrowheads) is devoid of staining, whereas the premigratory zone (pmz) is heavily labeled; in the mutant the whole egl is almost immunonegative. The molecular layer (ML) of the wild type is consistently B-50 positive but the presumptive molecular layer (PML) in the mutant shows only weakly labeled dots and fibers around Purkinje cell somata. Fibers in the white substance (WS) are immunopositive in both, but with a somewhat decreased intensity in the mutant. igl = internal granule cell layer. **C,D:** Five-month-old wild type and Weaver mutant: in the wild type remaining B-50 immunoreactivity is almost exclusively localized in the ML, whereas the PML of the mutant is nearly free of labeling. Very weakly labeled fibers of the WS are visible in both. GL = granule cell layer. × 83.6. Bar = 100 μm.

B-50 and the specificity of the antibodies in these various mouse strains of various ages and in different brain areas. The differences in staining intensity of lanes which received samples from the same strain (B6CBA: hemisphere in lanes 2 and 3; cerebellum in lanes 4 and 5; Weaver: hemisphere in lanes 8 and 9; cerebellum in lanes 6 and 7) reflect the various amounts of samples applied to the gel. Differences between lanes which received the same amounts but from different strains (compare lanes 4 and 7 or lanes 5 and 6) are likely to indicate relative differences in B-50 content and corroborate the immunocytochemical results. Differences between young and adult animals are also visible (data not shown).

DISCUSSION

Since the migration of granule cells occurs from P4 until P20 (Miale and Sidman, 1961) in the mouse, paralleled by the migration and synaptogenesis of inhibitory interneurons and the formation of synaptic contacts of cerebellar afferents (Woodward et al., 1971), practically all of these neurons and even Bergmann glial processes

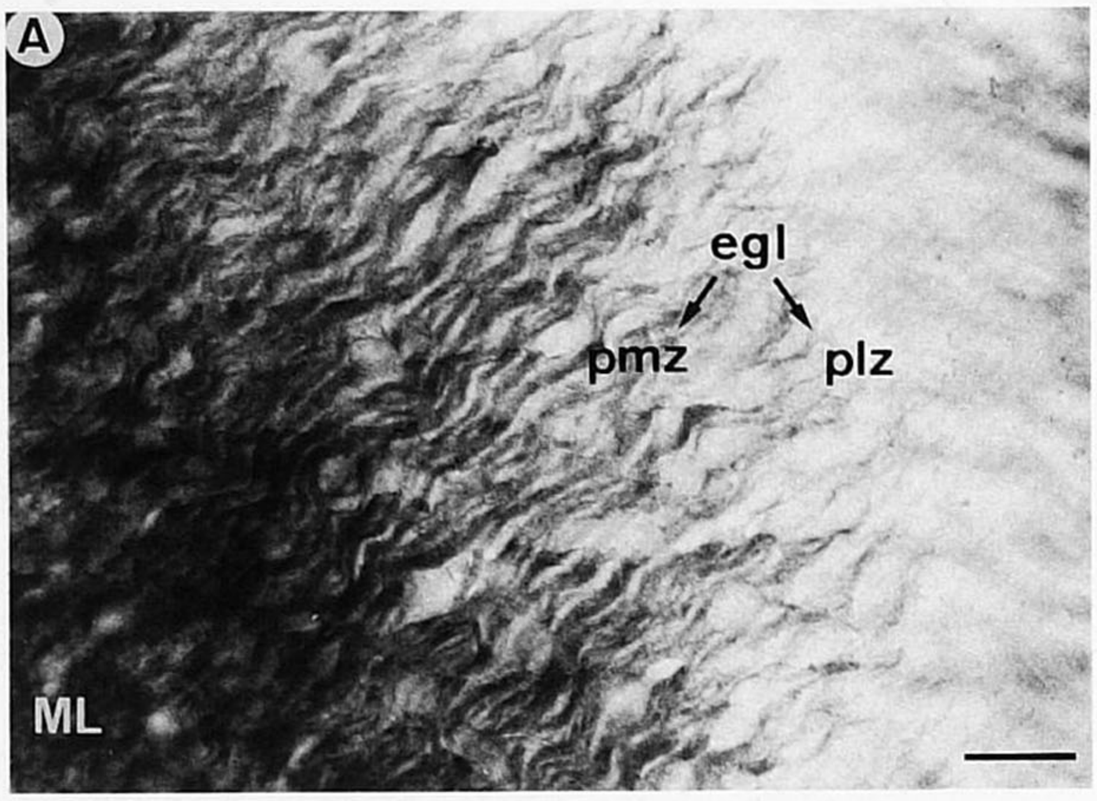

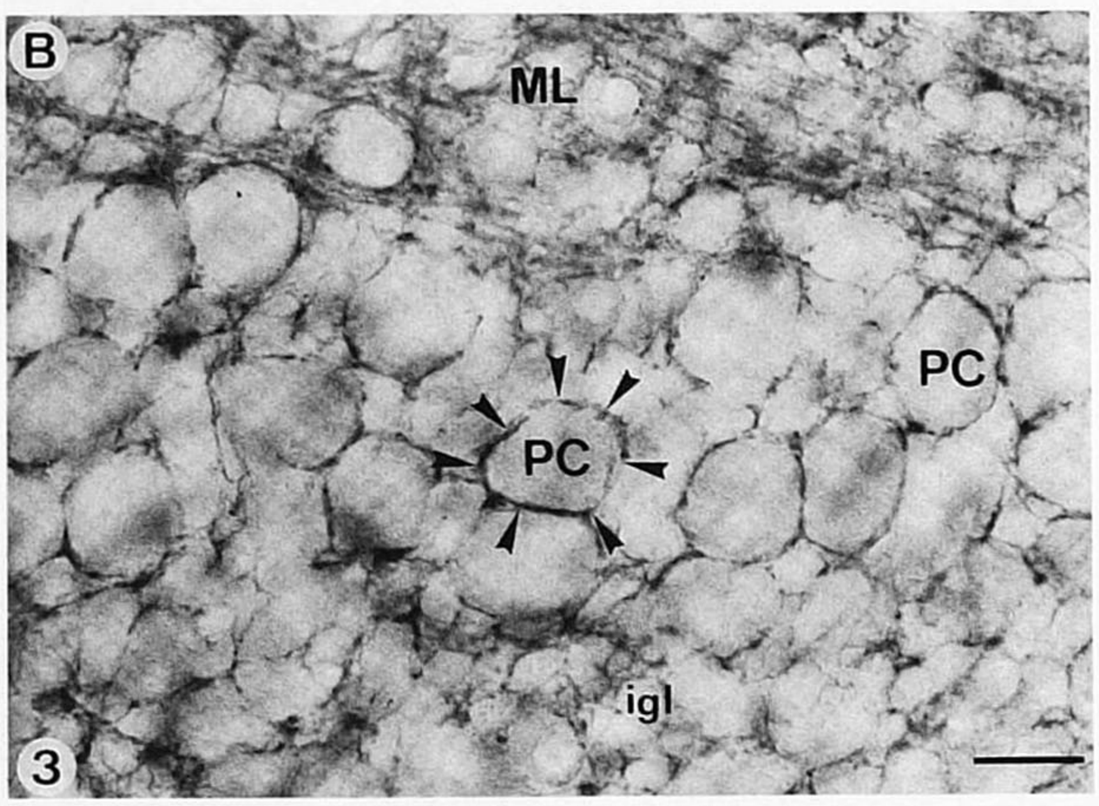

Fig. 3. Higher power view of the external granular layer (egl) (**A**) and the Purkinje cell (PC) layer (**B**) of a 10-day-old wild type immunostained with anti-B-50. **A:** Immunostained processes representing ''pioneer neurites'' of granule cells extend from the premigratory zone (pmz) of the egl into the molecular layer (ML), whereas the proliferative zone (plz) of the egl is unstained. **B:** Immunonegative somata of Purkinje cells are outlined by immunopositive dot- and fiber-like structures (arrowheads). igl = internal granule cell layer. × 550.9. Bars = 15.87 μm.

PCD-mutant *5 months*

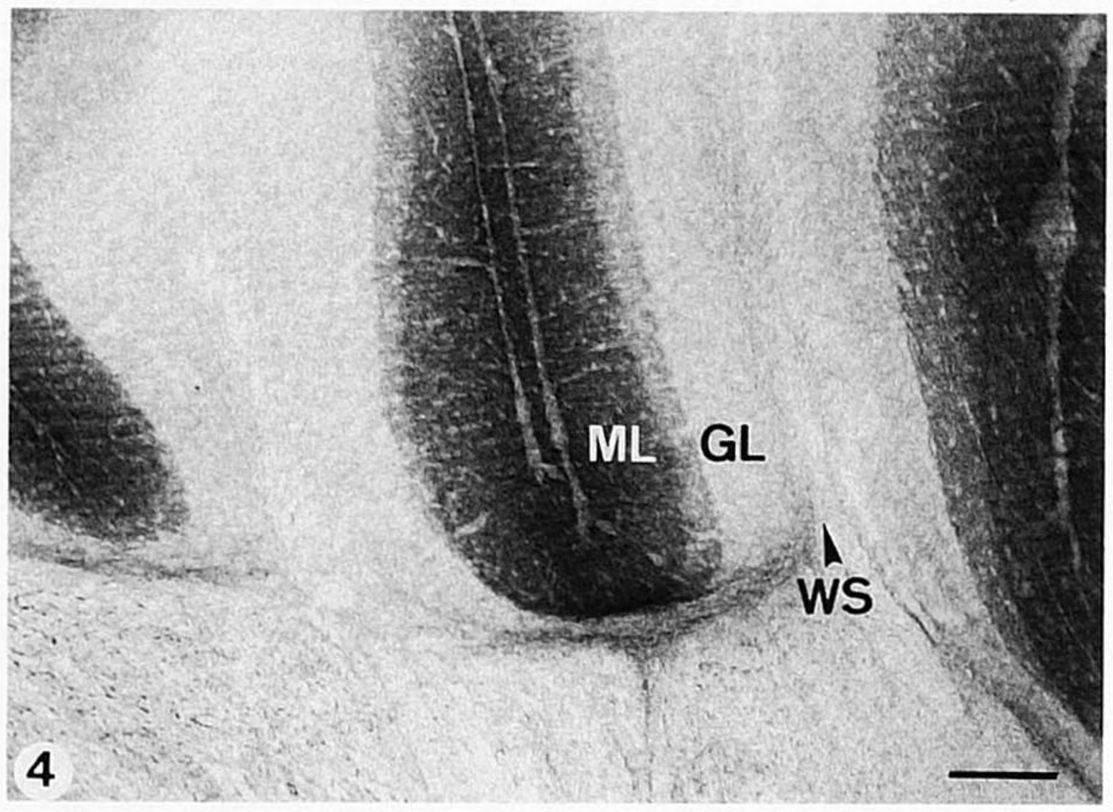

Fig. 4. B-50 immunoreactivity in the cerebellar cortex of a 5-month-old PCD-mutant. Dense reaction product is only found in the molecular layer (ML), and weak staining in the white substance (WS) is due to moderately labeled fibers. For comparison, see Figure 2C. GL = granule cell layer. × 87.4. Bar = 100 μm.

[although glial B-50 was only observed on rare occasions (Campbell et al., 1991)] are possible candidates for the B-50 immunolabeling in the ML of immature wild types. Nevertheless, the findings in mutants, where the granule cell loss occurs from P0 until about P20 (Smeyne and Goldowitz, 1989), allow a more precise localization of B-50 in the cerebellum. The almost complete absence of immunolabeling in the pmz, the drastic decrease of labeled elements in the pml of Weaver, and the heavy labeling and dense package of processes seen in the pmz and ML of young wild types, which appears again but with lower intensity in adult wild types and in immature and adult PCD-mutants, strongly suggest that these processes represent growing parallel fibers: 1) no parallel fibers are generated in Weaver due to the premigratory granule cell degeneration (Sotelo, 1982); 2) cerebellar afferents do not appear in the pmz (Palay and Chan-Palay, 1974); and 3) dependent on the plane of sectioning, these processes are also visible in a horizontal orientation which is never realized by Bergmann glial processes (Palay and Chan-Palay, 1974). Therefore, the dependency of B-50 expression on a regular granule cell migration and the outgrowth of parallel fibers rather than on the synaptogenesis of cerebellar interneurons is obvious. This is further supported by the results of in situ hybridization by Bendotti et al. (1991), who found B-50 mRNA only in the granule cell layer of the adult cerebellum, and by the present results obtained from Western blots.

The very few remaining B-50 positive structures in the pml of Weaver are scattered mainly around Purkinje cell bodies and therefore may represent climbing fiber contacts, which are known to retain their perisomatic localization in this mutant (Mariani, 1982). The marked labeling of fibers in the white matter supports this idea. Alternatively, pericellular nests of basket cells could be responsible for this labeling, but this could be questioned as these B-50 positive dots and fibers are missing in PCD-mutants, although it is known that empty baskets persist even in the absence of Purkinje cells (Sotelo,

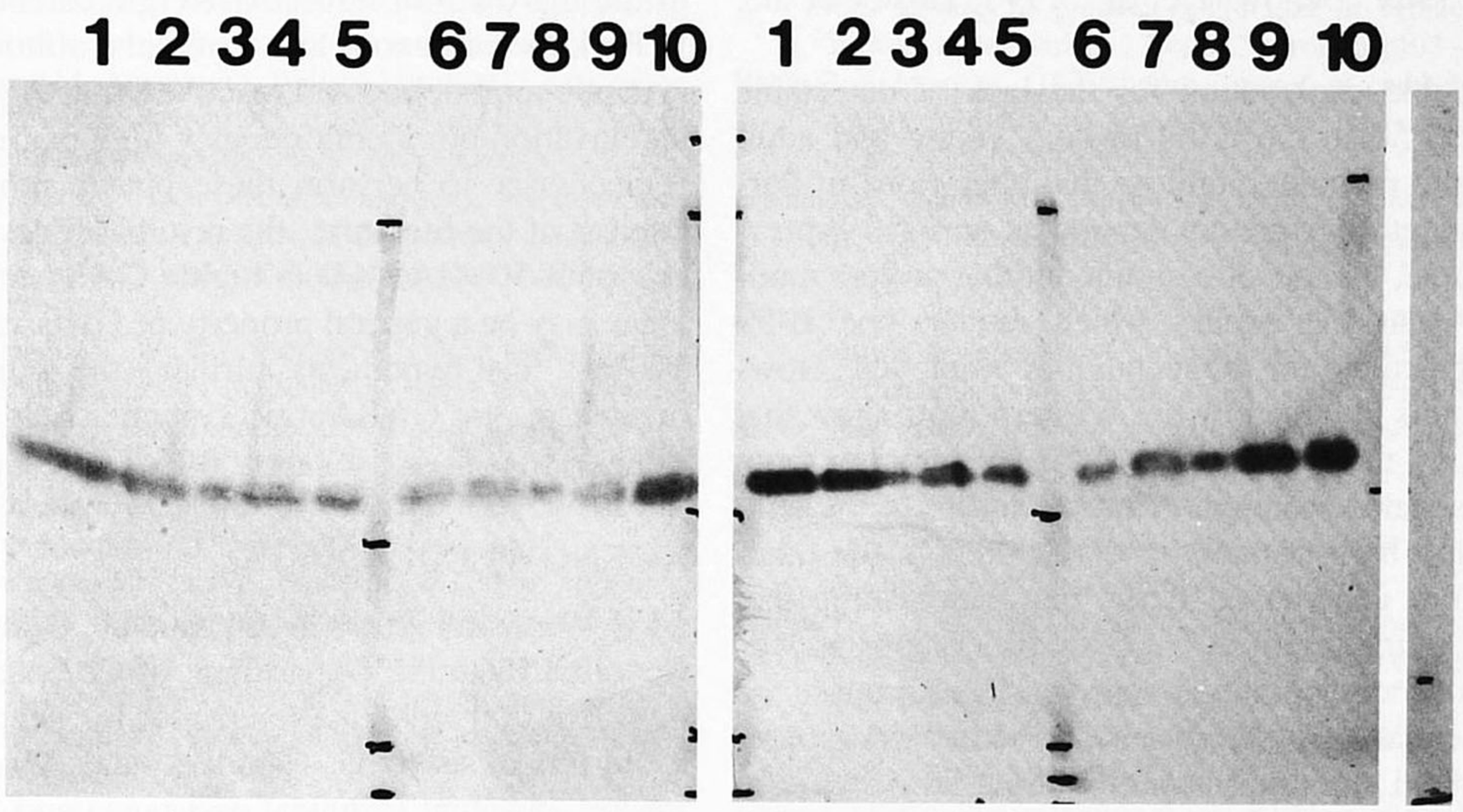

Fig. 5. Demonstration of the presence of B-50 in brain tissue homogenates of wild type (B6CBA) and Weaver mutant. The following samples were loaded on the gels of which the Western blots are shown: **lanes 1,10:** 25 μg protein of rat brain; **lanes 2,9** and **lanes 3,8:** 50 and 10 μg protein of mouse hemispheres, respectively; and **lanes 4,7** and **lanes 5,6:** 50 and 25 μg protein of mouse cerebellum, respectively. Samples in lanes 2–5 are derived from the B6CBA-wild type and samples in lanes 6–9 are from the Weaver mutant, both 6 months old. The **unnumbered lanes** contained the molecular mass markers. Black marks going from top to bottom of the blot indicate the molecular masses of 130, 75, 50, 39, and 27 kDa. The **left blot** was stained by the polyclonal antibodies, the **right blot** by the monoclonal B-50 antibodies, and the **strip** shows the control in which the primary antibody was omitted.

1980). In addition, a participation of monoaminergic afferents, which also contact Purkinje cell somata to a minor degree (Simon et al., 1979), cannot be excluded, as it is known that among the sources of cerebellar afferents the locus ceruleus and the nuclei of Raphé display the highest content of B-50 mRNA (Bendotti et al., 1991). A clear decision, however, is not possible in this case.

Since the spatial and intensity distribution of B-50 immunoreactivity in PCD-mice is similar to the corresponding controls, except for some missing immunoreactive dots in the former Purkinje cell row, the distribution of B-50 in the cerebellar cortex, the deep cerebellar and the vestibular nuclei does not appear to be affected by the loss of Purkinje cells. The heavily labeled fibers in the white matter of immature animals therefore do not contribute to Purkinje cell axons in PCD as well as in Weaver but to cerebellar afferents in neonatal mice.

Taken together, nearly all immunostained structures of the immature and the adult cerebellum in our material can be related to non-GABAergic neurons. A participation of B-50 in plastic processes at the terminal sites of the GABAergic Purkinje cell projection to the dorsal part of the LVN is therefore not very likely. The almost complete lack of B-50 labeling in this nucleus in all animals and at all stages investigated shows directly that the continuous synaptic remodeling over the entire lifetime of the animals which is evidenced for normal mice and Weaver mutants (Bäurle et al., 1992) and for normal rats (Sotelo and Palay, 1971) is not accompanied by an elevation of immunocytochemically detectable B-50. Moreover, the reinnervation of LVN giant neurons by GABAergic terminals observed in Weaver again does not seem to lead to an elevation of B-50 immunoreactivity in this nucleus in any way.

The question arises whether the timing of our investigation to detect changes in B-50 expression during the sprouting in Weaver was well chosen. The partial degeneration of Purkinje cells is believed to be already completed at P5, but it is not yet clarified to what extent this Purkinje cell loss occurs pre- or postnatally (Blatt and Eisenman, 1985). The first phenotypical signs of cerebellar ataxia are visible around P8–P10 in this mutant (Sidman et al., 1965). However, degeneration of nerve terminals and reinnervation of vacated postsynaptic space occur in a time interval of approximately 1 month (Nadler et al., 1974; Gilad and Reis, 1979; Goldowitz et al., 1982; Raisman, 1985; Katsumaru et al., 1986; Vuillon-Cacciuttolo et al., 1986), and elevated B-50 expression is reported to accompany or even outlast the whole period of axonal elongation and synaptogene-

sis (Skene, 1989; Benowitz et al., 1990; Doster et al., 1991).

A possible explanation for the lack of detectable amounts of B-50 in the LVN in both young and adult wild types and mutants might be that alterations in Purkinje cell synaptology are not dependent on B-50 expression. Of course, one never can rule out that protein modification or masking occurs which renders the B-50 protein undetectable for the techniques employed. However, the results obtained by the Western blots show that the antibodies used recognize B-50 in samples from hemispheres and cerebellum of rat as well as of the wild type mice and both mutants investigated. On the other hand, in more generalized terms one can assume that B-50 is not as important in GABAergic systems as was evidenced for monoaminergic neurons. In addition to the results presented here, there are also other systems in which collateral sprouting occurs without an increase in B-50 expression (Brown et al., 1992), and from other investigations it seems that in regions where the content of the inhibitory transmitter GABA is high, the level of B-50 is rather low. Oestreicher and Gispen (1986), investigating B-50 immunoreactivity in the adult hippocampus, observed that at sites between and near the somata of pyramidal and granule cells where inhibitory terminals of the intrinsic GABA neurons are concentrated (Storm-Mathisen, 1977), deposits of B-50 immunoreactivity are comparatively rare. Bendotti et al. (1991) found no B-50-mRNA signals in substantia nigra pars reticulata or the red nucleus, both of which are characterized by a high content of GABA and, at least in the case of the red nucleus, plasticity of GABAergic neurons is evidenced (Tsukahara et al., 1974; Nieoullon and Dusticier, 1981; Katsumaru et al., 1986). On the other hand, high B-50 expression in the adult is found in brain regions not considered areas of high plasticity and vice versa (for review see Skene, 1989). A suggestion that B-50 expression only plays a minor role, if at all, in GABAergic neuroplasticity can also be derived by comparing the separate studies of Goldowitz et al. (1982) and Benowitz et al. (1990) on neuroplastic changes after entorhinal cortex lesion in the adult rat. The time courses and the regional changes of glutamic acid decarboxylase (GAD) immunoreactivity (Goldowitz et al., 1982) and B-50 immunoreactivity (Benowitz et al., 1990) are quite different. While the changes in intrinsic GAD fiber distribution in the absence of the cholinergic septohippocampal pathway were still evident in the area dentata (Goldowitz et al., 1982), it is not known how B-50 immunoreactivity changes under these conditions.

In conclusion, the present results show that B-50 expression in the cerebellum is mainly attributable to the outgrowth of parallel fibers, for which a regular granule cell migration is the prerequisite, and, to a lesser extent, to the ingrowth of non-GABAergic cerebellar afferents. In Purkinje cell axons and terminals, although capable of synaptic remodeling and reactive synaptogenesis, neither an elevation nor a continuously high expression of B-50 is necessary to perform these plastic processes. In the context of the literature, the results suggest that the scarcity of B-50 (GAP-43) in highly GABAergic-innervated areas may be a general property of GABAergic circuitry. To test this hypothesis further, the other well-documented plastic GABAergic systems could be examined.

ACKNOWLEDGMENTS

We thank Prof. W.G. van de Grind, Biophysics Research Institute, Department of Comparative Physiology, Rijksuniversiteit Utrecht, for his generous hospitality to one of us (U.G.-C.). We thank Ms. H. Wolynski for her excellent technical assistance and Ms. J. Dames for her expert help with the English translation.

REFERENCES

Akers RF, Routtenberg A (1985): Protein kinase C phosphorylates a 47 M_r protein (F1) directly related to synaptic plasticity. Brain Res 334:147–151.

Aloyo VJ, Zwiers H, Gispen WH (1983): Phosphorylation of B-50 protein by calcium-activated phospholipid-dependent protein kinase and B-50 protein kinase. J Neurochem 41:649–653.

Andreasen T, Luetje K, Heideman CW, Storm DR (1983): Purification of a novel calmodulin binding protein from bovine cerebral cortex membranes. Biochemistry 22:4615–4618.

Bäurle J, Grüsser-Cornehls U (1992): Plasticity of Purkinje cell terminals in the Weaver mouse. Eur J Neurosci Suppl 5:214.

Bäurle J, Grover BG, Grüsser-Cornehls U (1992): Plasticity of GABAergic terminals in Deiters' nucleus of Weaver mutant and normal mice: A quantitative light microscopic study. Brain Res 591:305–318.

Bendotti C, Servadio A, Samanin R (1991): Distribution of GAP-43 mRNA in the brain stem of adult rats as evidenced by in situ hybridization: Localization within monoaminergic neurons. J Neurosci 11:600–607.

Benowitz LI, Routtenberg A (1987): A membrane phosphoprotein associated with neural development, axonal regeneration, phospholipid metabolism, and synaptic plasticity. TINS 10: 527–532.

Benowitz LI, Rodriguez WR, Neve RL (1990): The pattern of GAP-43 immunostaining changes in the rat hippocampal formation during reactive synaptogenesis. Mol Brain Res 8:17–23.

Blatt GJ, Eisenman LM (1985): A qualitative and quantitative light microscopic study of the inferior olivary complex of normal, Reeler, and Weaver mutant mice. J Comp Neurol 232:117–128.

Brodal A (1981): "Neurological Anatomy. In Relation to Clinical Medicine." 3rd Ed. New York: Oxford Universtiy Press.

Brown MC, Booth CM, Bisby MA, Tetzlaff W (1992): Motoneuron sprouting is not associated with increases in GAP-43 MRNA. Soc Neurosci Abstr 18:262.16.

Campbell G, Anderson PN, Turmaine M, Lieberman AR (1991):

GAP-43 in the axons of mammalian CNS neurons regenerating into peripheral nerve grafts. Exp Brain Res 87:67–74.

Doster SK, Lozano AM, Aguayo AJ, Willard MB (1991): Expression of the growth-associated protein GAP-43 in adult rat retinal ganglion cells following axon injury. Neuron 6:635–647.

Gilad GM, Reis DJ (1979): Neurochemical plasticity: Increased glutamic acid decarboxylase activity in the olfactory tubercle following olfactory bulb removal during postnatal development. Brain Res 177:200–203.

Goldowitz D, Vincent SR, Wu J-Y, Hökfelt T (1982): Immunohistochemical demonstration of plasticity in GABA neurons of the adult rat dentate gyrus. Brain Res 238:413–420.

Jacobson RD, Virág I, Skene JHP (1986): A protein associated with axon growth, GAP-43, is widely distributed and developmentally regulated in rat CNS. J Neurosci 6:1843–1855.

Katsumaru H, Murakami F, Wu J-Y, Tsukahara N (1986): Sprouting of GABAergic synapses in the red nucleus after lesions of the nucleus interpositus in the cat. J Neurosci 6:2864–2874.

Katz F, Ellis L, Pfenninger KH (1985): Nerve growth cones isolated from fetal rat brain. III. Calcium-dependent protein phosphorylation. J Neurosci 5:1402–1411.

Mariani J (1982): Extent of multiple innervation of Purkinje cells by climbing fibers in the olivocerebellar system of Weaver, Reeler, and Staggerer mutant mice. J Neurobiol 13:119–126.

Mercken M, Lubke U, Vandermeeren M, Gheuens J, Oestreicher AB (1992): Immunocytochemical detection of the growth-associated protein B-50 by newly characterized monoclonal antibodies in human brain and muscle. J Neurobiol 23:309–321.

Miale I, Sidman RL (1961): An autoradiographic analysis of histogenesis in the mouse cerebellum. Exp Neurol 4:277–296.

Mullen RJ, Eicher EM, Sidman RL (1976): Purkinje cell degeneration, a new neurological mutation in the mouse. Proc Natl Acad Sci USA 73:208–212.

Nadler JV, Cotman CW, Lynch GS (1974): Biochemical plasticity of short-axon interneurons: Increased glutamate decarboxylase activity in the denervated area of rat dentate gyrus following entorhinal lesion. Exp Neurol 45:403–413.

Neve RL, Finch EA, Bird ED, Benowitz LI (1988): Growth-associated protein GAP-43 is expressed selectively in associative regions of the adult human brain. Proc Natl Acad Sci USA 85: 3638–3642.

Nieoullon A, Dusticier N (1981): Increased glutamate decarboxylase activity in the red nucleus of the adult cat after cerebellar lesions. Brain Res 224:129–139.

Oestreicher AB, Gispen WH (1986): Comparison of the immunocytochemical distribution of the phosphoprotein B-50 in the cerebellum and hippocampus of immature and adult rat brain. Brain Res 375:267–279.

Oestreicher AB, Van Dongen CJ, Zwiers H, Gispen WH (1983): Affinity purified anti-B-50 protein antibody: Interference with the function of the phosphoprotein B-50 in synaptic plasma membranes. J Neurochem 39:683–692.

Palay SL, Chan-Palay V (1974): ''Cerebellar Cortex. Cytology and Organization.'' Berlin: Springer.

Raisman G (1985): Synapse formation in the septal nuclei of adult rats. In Cotman CW (ed): ''Synaptic Plasticity.'' New York: Guilford, pp 13–38.

Rakic P, Sidman RL (1973a): Sequence of developmental abnormalities leading to granule cell deficit in cerebellar cortex of Weaver mutant mice. J Comp Neurol 152:103–132.

Rakic P, Sidman RL (1973b): Organization of cerebellar cortex secondary to deficit of granule cells in Weaver mutant mice. J Comp Neurol 153:133–162.

Sidman RL, Green MC, Appel SH (1965): ''Catalog of the Neurological Mutants of the Mouse.'' Cambridge: Harvard University Press.

Simon H, Le Moal M, Calas A (1979): Efferents and afferents of the ventral tegmental A-10 region studied after local injection of [^{3}H]leucine and horseradish peroxidase. Brain Res 175:1–23.

Skene JHP (1989): Axonal growth-associated proteins. Annu Rev Neurosci 12:127–156.

Skene JHP, Willard M (1981): Axonally transported proteins associated with axon growth in rabbit central and peripheral nervous systems. J Cell Biol 89:96–193.

Smeyne RJ, Goldowitz D (1989): Development and death of external granular layer cells in the Weaver mouse cerebellum: A quantitative study. J Neurosci 9:1808–1820.

Sotelo C (1980): Mutant mice and the formation of cerebellar circuitry. TINS 3:33–36.

Sotelo C (1982): Synaptic remodeling in agranular cerebella. In Palay SL, Chan-Palay V (eds): ''The Cerebellum—New Vistas.'' New York: Springer, pp 50–68.

Sotelo C, Palay SL (1971): Altered axons and axon terminals in the lateral vestibular nucleus of the rat. Possible example of axonal remodeling. Lab Invest 25:653–671.

Sternberger LA, Hardy LA Jr, Cuculis JJ, Meyer HG (1970): The unlabelled antibody method of immunohistochemistry. Preparation and properties of soluble antigen complex and its use in identification of spirochetes. J Histochem Cytochem 18:315–333.

Storm-Mathisen J (1977): Localization of transmitter candidates in the brain: The hippocampal formation as a model. Prog Neurobiol 8:119–181.

Towbin H, Staehelin T, Gordon J (1979): Electrophoretic transfer of proteins from polyacrylamide gels to nitrocellulose sheets: Procedure and applications. Proc Natl Acad Sci USA 76:1979–1982.

Tsukahara N, Hultborn H, Murakami F (1974): Sprouting of corticorubral synapses in red nucleus neurones after destruction of the nucleus interpositus of the cerebellum. Experientia 30:57–58.

Vuillon-Cacciuttolo G, Bosler O, Nieoullon A (1986): Immunohistochemical evidence of plasticity of gamma-aminobutyric acid neurons in the red nucleus and adjacent reticular formation after contralateral cerebellectomy in the adult cat. Neurosci Lett 70: 308–313.

Wassef M, Simons J, Tappaz ML, Sotelo C (1986): Non-Purkinje cell GABAergic innervation of the deep cerebellar nuclei: A quantitative immunocytochemical study in C57BL and in Purkinje cell degeneration mutant mice. Brain Res 399:125–135.

Woodward DJ, Hoffer BJ, Siggins GR, Bloom FE (1971): The ontogenetic development of synaptic junctions, synaptic activation and responsiveness to neurotransmitter substances in rat cerebellar Purkinje cells. Brain Res 34:73–97.

Zwiers H, Schotman P, Gispen WH (1980): Purification and some characteristics of an ACTH-sensitive protein kinase and its substrate protein in rat brain. J Neurochem 34:1689–1699.

Journal of Neuroscience Research 38:336–347 (1994)

Reactive Astrocytes Are Widespread in the Cortical Gray Matter of Amyotrophic Lateral Sclerosis

D. Nagy, T. Kato, and P.D. Kushner

ALS and Neuromuscular Research Foundation, California Pacific Medical Center, San Francisco

The distribution of reactive astrocytes was examined in the cortical gray matter of non-motor and motor regions from cases of familial and sporadic amyotrophic lateral sclerosis (ALS) and compared to that of β-amyloid deposits. By glial fibrillary acidic protein immunocytochemistry, patches of reactive astrocytes, characterized by multiple reactive astrocytes in a circular or patch-like formation, occurred in 12 of 15 ALS cases examined. These patches of reactive astrocytes were not restricted to the motor cortex but were found in the gray matter in ALS in all examined brain regions, including frontal, temporal, inferior parietal, cingulate, occipital, and motor cortices, from both familial and sporadic ALS cases. Reactive astrocytes were also found in the subpial region and at the gray/white matter junction. Because patches of astrocytes can occur in association with senile plaques, β-amyloid was localized. By immunostaining, β-amyloid deposits were observed in five of the 15 ALS cases: three cases had only early plaques, two had both early and classic plaques. The number of ALS cases with both astrocyte patches and amyloid plaques was four of 15, but typically astrocyte patches in ALS occurred without any evidence of an association with β-amyloid deposits. Therefore, the astrocyte patches in ALS are not the result of β-amyloid deposition. The widespread occurrence of reactive astrocytes, as patches in the cortical gray matter and in the subpial region and at the gray/white matter junction, is evidence of a widespread pathology in ALS cortex in both familial and sporadic forms of the disease.

Key words: glial fibrillary acidic protein, Alzheimer's disease, β-amyloid protein, neuropathology

INTRODUCTION

Both familial and sporadic forms of amyotrophic lateral sclerosis (ALS) are characterized by the degeneration of both upper and lower motor neurons, as revealed by clinical evaluations (reviewed by Rowland, 1991) and neuropathological examinations (e.g., Davison, 1941; Hammer et al., 1979; Lawyer and Netsky, 1953). Recent studies have described reactive changes in astrocytes occurring in the gray matter in the motor cortex in ALS. Using immunocytochemical methods, Kamo et al. (1987) described patches of astrocytes within the primary motor cortex, in LII-III and sometimes in LIV-V, the site of the Betz cells. Murayama et al. (1991) confirmed the presence of these patches, in the primary motor cortex.

In contrast to these studies of the motor cortex, we reported an astrogliosis in the superficial subcortical white matter in ALS that was widespread, occurring in multiple cortical areas, with no restriction to or obvious increase in the motor region (Kushner et al., 1991). Because of this widespread distribution of reactive astrocytes of the white matter, it seemed possible that the reported patches of astrocytes might likewise have a widespread distribution in ALS. Therefore, the aim of the present study was to examine the pattern of reactive astrocytes in the gray matter of ALS cases in multiple cortical regions. We analyzed samples from both familial and sporadic forms of ALS and have emphasized our results from the two forms in view of any possible differences in the neuropathology of familial ALS, most cases of which have been found to have a defect in the gene encoding copper, zinc superoxide dismutase (Rosen et al., 1993).

Patches of astrocytes can occur in association with

Received April 21, 1993; revised November 22, 1993; accepted November 23, 1993.

Address reprint requests to P.D. Kushner, 1362 6th Avenue, San Francisco, CA 94122.

D. Nagy is presently at Somatix Therapy Corporation, 850 Marina Village Parkway, Alameda, CA 94501.

T. Kato is presently at Yamagata University, School of Medicine, Yamagata 990-23, Japan.

P.D. Kushner is presently at Department of Biology, Cell Biology Division, San Francisco State University, 1600 Holloway Ave., San Francisco, CA 94132.

β-amyloid deposits (e.g., Harpin et al., 1990; Rozemuller et al., 1989; Shimada et al., 1991). We thus explored the possibility of a correlation of the astrocytic patches in ALS with β-amyloid deposits. It should be noted that intellectual impairment is not usually considered one of the clinical symptoms of ALS, although there are several reports describing individual ALS patients with intellectual impairment, cognitive function deficit, or even severe dementia, in addition to the typical clinical signs of motor neuron disease (Hirano, 1991; Horoupian et al., 1984; Iwasaki et al., 1990; Mitsuyama and Takamiya, 1979; Myrianthopoulos and Smith, 1962; Wikstrom et al., 1982). Because astrocyte patches can occur in association with amyloid deposits, it seemed important to address the possibility of amyloid deposits directly. Additionally, ALS-parkinsonism-dementia-complex is well known to occur among the Chamorros on Guam (Rodgers-Johnson et al., 1986).

MATERIALS AND METHODS

Tissues Used

The cases used for this study totalled 31: 15 ALS cases and 16 control cases, including seven neurologically normal cases, seven neurologically diseased cases, and two cases of Alzheimer's disease (AD), as positive controls for β-amyloid staining. Most of these specimens were also used for a previous study on subcortical astrogliosis in ALS (Kushner et al., 1991). Specimens from two familial (ALS3 and ALS5) and 10 sporadic ALS cases were obtained through the cooperation of Dr. F.H. Norris and the Pathology Department of the California Pacific Medical Center (CPMC). One sporadic case of ALS was obtained from the Humboldt Central Laboratory, Eureka, CA. Two additional cases were provided by Dr. W. Tourtellotte, National Neurological Research Bank (NNRB), Veterans Administration Medical Center, Wadsworth Division, Los Angeles, CA. Ten of the ALS cases had clinical histories of both upper and lower motor neuron involvement. One ALS case (ALS1) had bulbar ALS; one case (ALS15) had primary lateral sclerosis. Both familial ALS cases had symptoms of classic ALS, with no multisystem degeneration. Seven non-neurologically diseased cases (three cases of heart disease, one case of liver disease, three cases of carcinoma) were obtained from CPMC. The seven neurologically diseased cases included one case of seizures (CPMC), two cases of multiple sclerosis (MS) (NNRB), one case of multiple infarction (NNRB), one case of Parkinson's disease (PD) (NNRB), one case of Pick's disease (NNRB), and one case of atherosclerotic coronary artery disease (ASCAD) with an old infarction in the contralateral cortex (CPMC). One case of AD was provided by Dr. R. Terry (University of California, San Diego), the other AD case by the NNRB. Diagnosis was determined by clinical criteria and confirmed by pathological examination at the source institution. For the ALS cases, ages ranged from 39 to 78 years (mean 58 years); the postmortem delay interval (PMDI) ranged from 2 to 52 hr (mean 11 hr). For the non-neurologically diseased cases, ages ranged from 50–88 years (mean 65 years), PMDI 5.5–115 hr (mean 35.5). For the neurologically diseased cases, ages ranged from 63–86 years (mean 74 years), PMDI 3–14 hr (mean 7 hr). The ages of the AD cases were 94 years and 77 years (mean 85.5 years); PMDIs were not available.

Regions Examined

Blocks of isocortex were excised from formalin-fixed brains as follows: Midfrontal cortex (10 ALS cases, 14 control cases), approximately 10 cm caudal to the frontal pole and, from the superior temporal gyrus, halfway between the foot of the central sulcus and the temporal pole; inferior parietal cortex (two ALS cases, two control cases), 1 cm caudal and 2 cm posterior to the foot of the lateral fissure; motor cortex (eight ALS cases, one control case), 1 cm rostral to the central sulcus and 4 cm lateral to the longitudinal fissure; cingulate cortex (two ALS cases), 1 cm superior to the corpus callosum and 6 cm caudal to the frontal pole; temporal cortex (four ALS cases), 2 cm above the base of the temporal pole on the lateral hemisphere; occipital cortex (two ALS cases, one control case), 1 cm lateral to the occipital pole. Blocks were superficial; they did not include areas of centrum semiovale and ventricular white matter and most probably excluded U fibers.

Tissue Processing

To heighten immunoreactivity and to avoid freezing artefacts, formalin-fixed tissue blocks were processed as described previously (Kushner et al., 1989, 1991). Briefly, fixed blocks, stored at 4°C, were rinsed in a large volume of phosphate buffered saline (PBS) and equilibrated through cold, aqueous graded sucrose solutions, 12% (24 hr), 15% (24 hr), and 18% (24–76 hr) sucrose. These steps optimize antigenicity and reduce freezing artifact. Blocks were mounted in gum tragacanth with the orientation that allowed an examination of a maximum area of gray and white matter within each tissue section. Mounted blocks were flash frozen in liquid nitrogen-cooled isopentane, stored at −70°C, and cryosectioned at 10 μm. Near-adjacent sections were routinely stained with hematoxylin and eosin (H & E) and thioflavin-S and by a modified Bielschowsky technique. Three samples of motor cortex could not be identified as motor cortex on the basis of cytoarchitecture (Betz cells and agraunularity) in H & E stained sections,

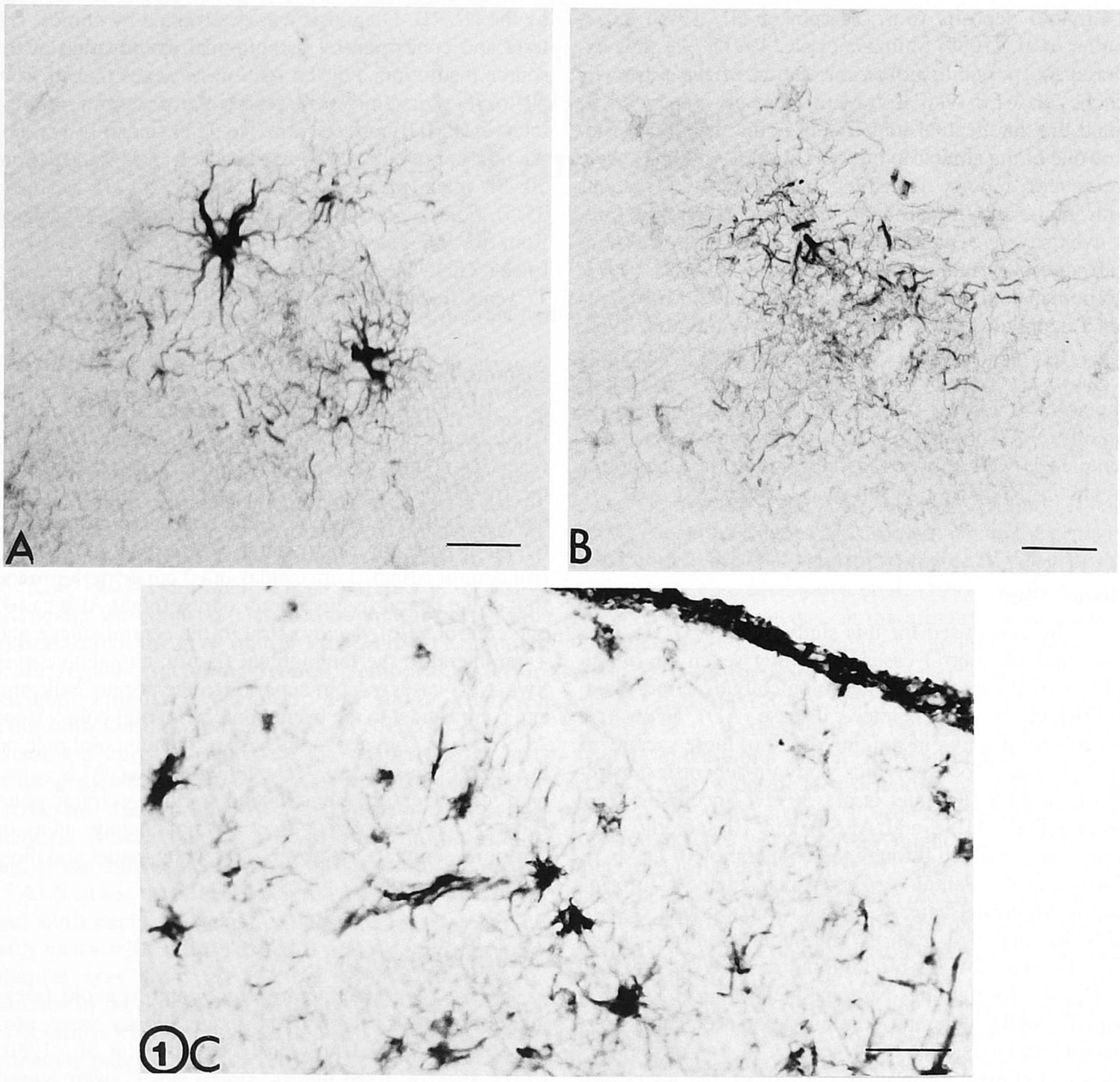

Fig. 1. Reactive astrocytes in the gray matter in ALS demonstrated by GFAP immunostaining. **A:** A typical patch of GFAP-positive astrocytes in the frontal cortex of ALS brain (LIII). **B:** Circular-appearing GFAP-positive processes without any apparent astrocyte cell body (fiber patch) in ALS frontal cortex (LII). **C:** Reactive astrocytes in the subpial region and in LI-II in ALS motor cortex. **D:** Astrocytosis at the gray-white matter junction with finger-like extensions up into LVI in ALS temporal cortex. gm, gray matter; wm, white matter. Bar = 30 μm.

while five cases (ALS1, ALS3, ALS5, ALS6, ALS8) were positively identified as motor cortex.

Immunocytochemistry

For both β-amyloid and glial fibrillary acidic protein (GFAP) staining, sections were briefly hydrated in PBS and then incubated in a 0.3% H_2O_2 solution to block endogenous peroxidase.

For GFAP staining we used rabbit anti-GFAP (specific for GFAP, with no crossreactivity to vimentin, Biogenex Labs, San Ramon, CA) and a peroxidase anti-peroxidase system (Biogenex Labs) and 3,3-diaminobenzidine (DAB) for visualization.

The antisera to β-amyloid protein fragments were kindly provided by Drs. D. Selkoe (Brigham and Women's Hospital, Boston) and G. Cole (University of Cali-

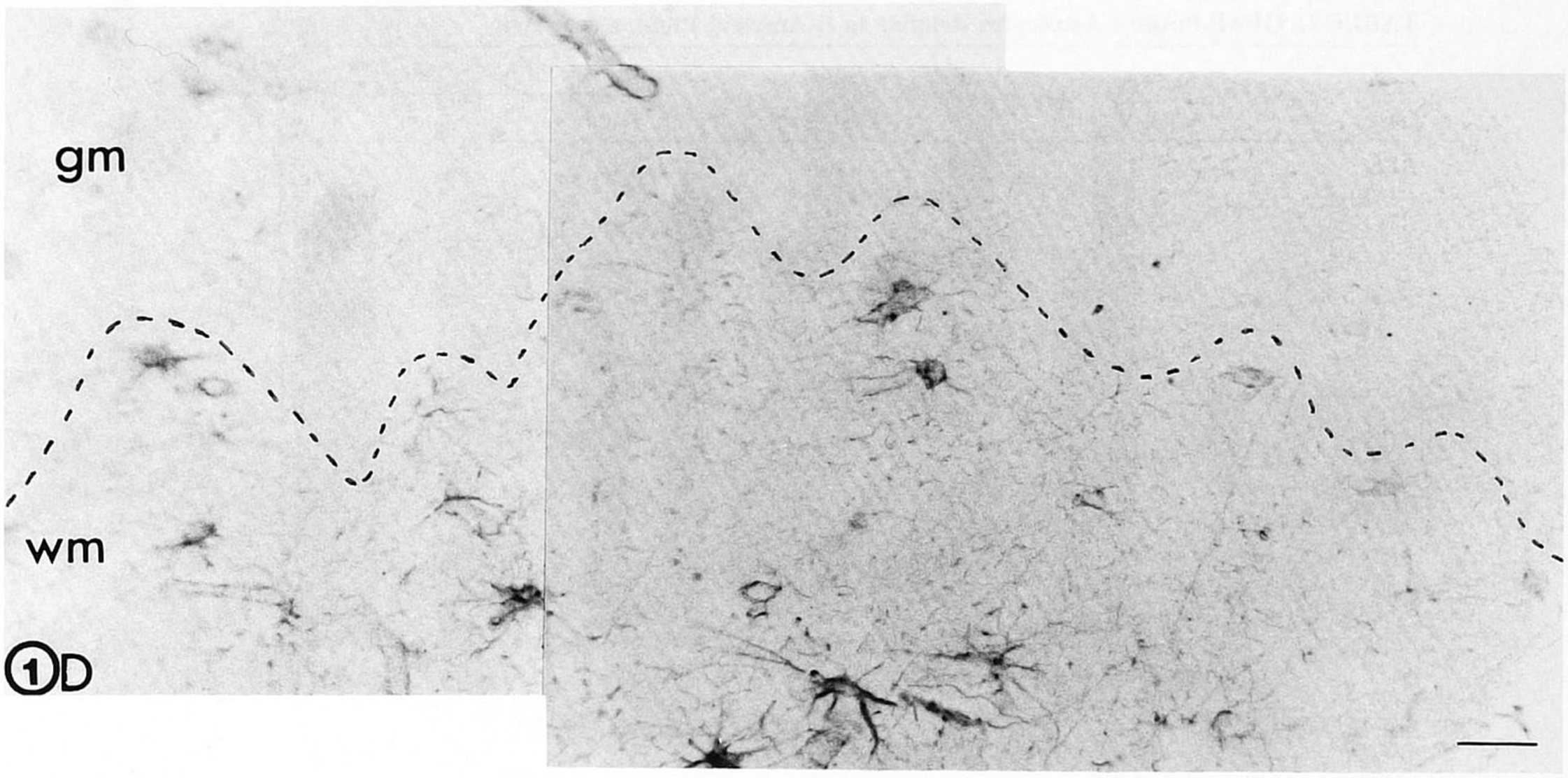

Fig. 1D.

fornia, San Diego). The antisera were made to synthetic β-amyloid peptides, amino acids 1–38, antiserum 1280 (Joachim et al., 1989), and amino acids 14–28, anti-β-14-28 (Cole et al., 1989).

Immunocytochemical staining for β-amyloid protein was enhanced by pretreatment of the tissue sections with 80% formic acid (Kitamoto et al., 1987). The antiserum 1280 was diluted 1:1,000 in PBS; the anti-β-14-28 was diluted 1:500 in PBS containing 0.05% Triton-X 100. To prevent non-specific staining, after the incubation with the primary antisera, sections were incubated for 5 min in 5% casein. Antibody binding was visualized with an avidin/biotin peroxidase system (Vector ABC-KIT, Vector Labs., Burlingame, CA) and DAB.

Sections were dehydrated, mounted in synthetic mounting medium, and examined under normal light with a Zeiss Ultraphot microscope.

Evaluation and Quantitation of Stained Sections

Sections of cortical samples measured approximately 1 × 1 cm and contained the glial limitans, gray matter, and some superficial white matter. Sections were scored for patches and plaque deposits by examining the total cross sectional area of stained sections (four to six sections per region). AD cases served as positive control for β-amyloid plaques. Cases with β-amyloid deposits typically had approximately six plaques/section, early or classic.

RESULTS

In the present study 15 ALS and 16 control cases were examined for astrogliosis; two of the ALS cases were of the familial form. Areas examined included primarily the cortical gray matter from motor, frontal, and temporal cortices and, in some cases, inferior parietal, cingulate, and occipital cortices. Formalin-fixed, near-adjacent cryosections were stained with H & E for cytoarchitectural evaluation and immunostained with either anti-GFAP or anti-β-protein. Modified Bielschowsky and thioflavin-S stains were used to evaluate the β-amyloid immunostaining.

GFAP Staining

An examination of motor, frontal, temporal, and, in two cases, inferior parietal, cingulate, and occipital cortices revealed patches of reactive astrocytes in 12 of 15 ALS cases, including both of the familial ALS cases. Patch-positive samples typically had three to five patches/section. Two different types of patches were observed. One type was characterized by multiple clusters of reactive astroglia, containing two to eight astrocytes per cluster (Fig. 1A) and was found in six cases (average age at death, 56 years). The other type of patch consisted of many GFAP-positive fibers in a circular configuration, without any apparent glia cell body. This was presumably due to the level of sectioning and was probably a patch at another level; we termed these patches with no cell body fiber-patches (Fig. 1B). Fiber-patches were

TABLE I. GFAP-Positive Astrocytes Relative to β-Amyloid Immunoreactivity

			GFAP ± patches β-amyloid			
Case	Age (yr)/Sex	Diagnosis	Patch	Fiber-patch	Early	Classic
ALS						
ALS1	55/F	ALS/bulbar	+	−	+	+
ALS2	59/M	ALS	+	−	+	+
ALS3	53/M	ALS/familial	+	+	−	−
ALS4	63/M	ALS	−	+	+	−
ALS5	49/F	ALS/familial	+	−	−	−
ALS6	39/F	ALS	+	+	−	−
ALS7	44/M	ALS	+	−	−	−
ALS8	60/M	ALS	+	−	−	−
ALS9	61/M	ALS	−	−	−	−
ALS10	67/M	ALS	−	+	+	−
ALS11	70/M	ALS	+	−	−	−
ALS12	51/M	ALS	−	+	−	−
ALS13	63/M	ALS[a]	−	−	−	−
ALS14	64/M	ALS	−	−	+	−
ALS15	78/M	primary lateral sclero.	+	+	−	−
	avg. 58.4 yr (± 9.8)		9/15	6/15	5/15	2/15
Normal control						
C1	67/M	adenoca.	−	−	+	−
C2	65/F	squam. cell ca.[a]	−	−	−	−
C3	67/M	cirrh. hepat.	−	−	−	−
C4	67/M	lung ca.[b]	−	−	−	−
C5	88/M	CHF	−	−	−	−
C6	50/M	cardiomyopathy[a]	−	−	−	−
C7	50/F	cardiopulm. arrest	−	−	−	−
	avg. 65 yr (± 12)		0/7	0/7	1/7	0/7
Neurological control						
NC1	63/M	seizures	−	−	+	−
NC2	79/M	PD	−	−	−	−
NC3	65/F	MS	+	+	+	−
NC4	59/M	MS	−	−	−	−
NC5	93/F	Pick's	+	+	+	+
NC6	71/F	multiinfarct.	+	+	+	+
NC7	83/M	ASCAD[a]	+	+	+	+
	avg. 73.3 yr (± 11.3)		4/7	4/7	5/7	3/7
Positive control						
AD1	94/M	AD/multiinfarct.	+	−	+	+
AD2	77/F	AD	+	+	+	+
	avg. 85.5 yr		2/2	2/2	2/2	2/2

GFAP-positive astrocytes relative to β-amyloid immunoreactivity in the cerebral cortex of ALS and control cases. When patches and/or plaques were present in one specimen they were found also in all specimens from that case. Analysis: sections of all cases and all regions were analyzed microscopically and scored for astrocyte patches and β-amyloid deposits in the gray matter. Cases were scored as positive if they had three to five astrocyte patches/section and a minimum of six plaques/section, early and/or classic. adenoca., adenocarcinoma; squam. cell ca., squamous cell carcinoma (case C2, of the mouth); cirrh. hepat., cirrhosis hepatitis; lung ca., lung carcinoma; CHF, chronic heart failure; cardiopulm. arrest, cardiopulmonary arrest; PD, Parkinson's disease; MS, multiple sclerosis; Pick's, Pick's disease; multiinfarct., multiple cerebral infarction; ASCAD, atherosclerotic coronary artery disease; AD, Alzheimer's disease.

[a]These cases had a diffuse gliosis, including ALS13.

[b]Focal gliosis in LII-III.

found in three cases (average age, 60 years). In an additional three cases (average age, 57 years) patches and fiber-patches occurred together (see Table I).

The distribution of astrocyte patches in ALS displayed a unique laminar pattern in the cortex that varied according to region (Fig. 2). In the motor cortex, patches occurred in layer LII in approximately 70% of the patch-containing cases; patches in LIII were found in approximately 45% of these cases and in LV in approximately 30%. In contrast, in the frontal cortex, only 10% of the

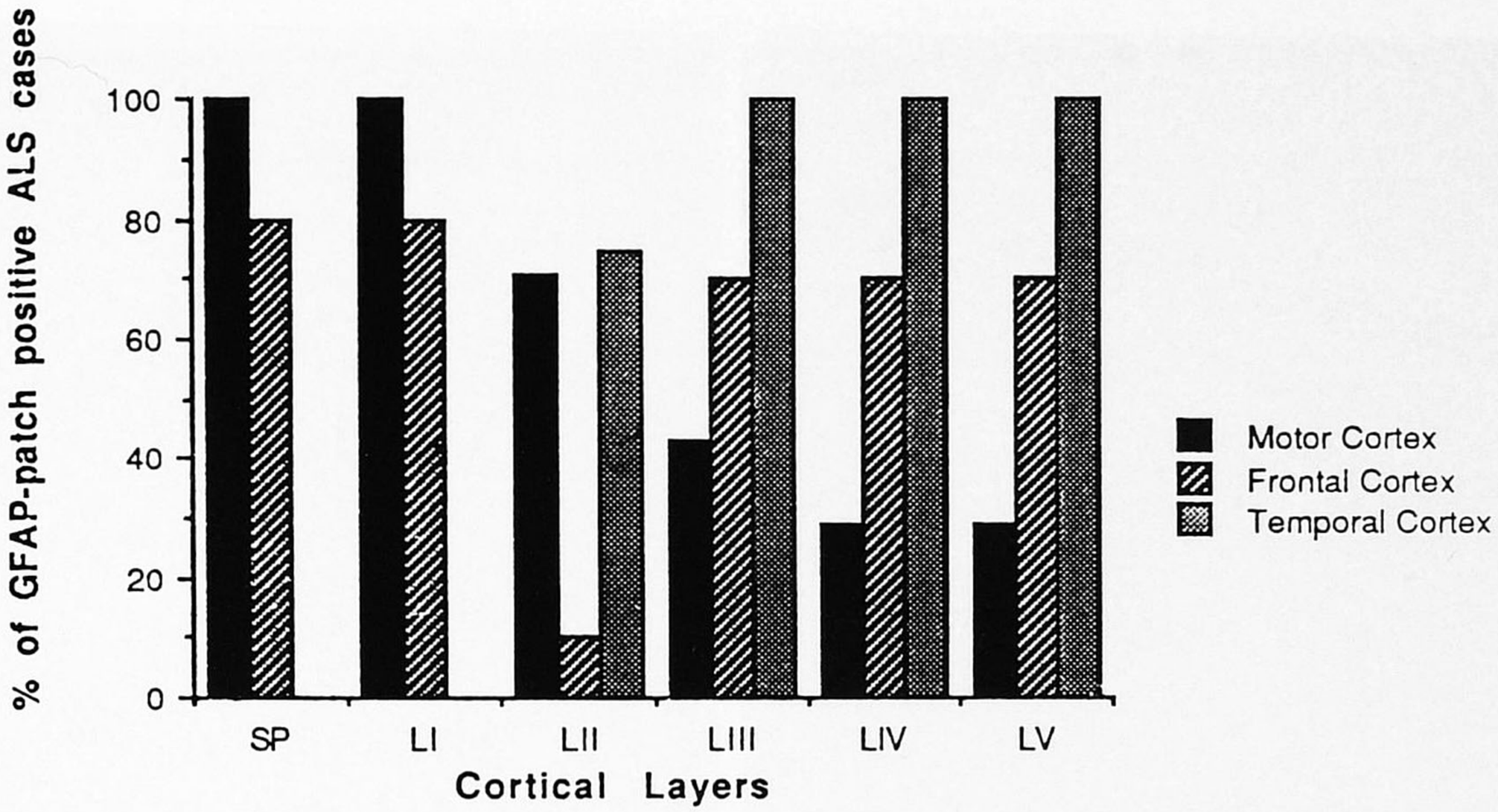

Fig. 2. Distribution of GFAP-positive patches in ALS cortex according to the cortical region and laminar structure. GFAP-positive patches predominate in the shallow layers in the motor cortex and in the deeper layers in other cortices. This figure was generated by the evaluation of four to six sections of each ALS case and region examined.

patch-containing cases had patches in LII, and the majority (approximately 70%) of the cases had patches in the deeper layers (LIII, LIV, and LV). In the temporal cortex, the pattern was similar to that found in the frontal cortex: patches occurred in LII in 75% of the cases and in LIII-IV and V in 100%. There was no obvious morphological difference to account for the laminar patterns.

Two other sites of reactive astrogliosis were detectable in the gray matter of ALS cortex. First, there was an increased number of reactive astrocytes in the subpial region, extending into the molecular layer (LI), in 13 of 15 cases, including both cases of the familial form of ALS. In most of these cases the reactive astrocytes and their processes formed a darkly staining band on the surface of the brain (Fig. 1C). Second, there was an enhanced astrogliosis that seemed to be an extension of the previously described subcortical white matter astrogliosis (Kushner et al., 1991) that extended, in finger-like formations, up into LVI and occasionally LV in 11 of 15 ALS cases (Fig. 1D). Additionally, one ALS case (ALS13) had a diffuse gliosis throughout the gray matter.

Three different control groups were used for comparison: non-neurologically diseased cases, neurologically diseased cases, and two AD cases as positive controls for β-amyloid staining. None of the seven non-neurologically diseased cases examined had patches of reactive astrocytes (Fig. 3A). There were no reactive astrocytes in the subpial region in five of these seven cases, and there were no visible finger-like formations of reactive astrocytes at the gray/white matter interface. The two cases (C2 and C6, 65 years and 50 years, respectively) with reactive astrocytes in the subpial region also had a diffuse gliosis throughout the gray matter (Fig. 3B). One of these cases had a history of chronic heart disease (C6, cardiomyopathy), while the other had a squamous cell carcinoma of the mouth with no apparent cerebral involvement (C2).

In the neurologically diseased control group (average age at death, 73 years), three of seven cases displayed no astrocyte patches. In the four patch-containing cases (NC3 = 65 years, NC5 = 93 years, NC6 = 71 years, NC7 = 83 years) the patches were diffusely distributed in all layers and occasionally were confluent, in contrast to the ALS cases where a laminar distribution was evident. In three cases, there was no notable evidence for reactive astrocytes in the subpial region. In none of the seven neurologically diseased cases were there reactive astrocytes in LV-VI or at the gray/white matter interface. Reactive astrocytes in the subpial region and astrocyte patches occurred together in the one case of Pick's disease that was examined (NC5, frontal cortex) (Fig. 3C). The two AD cases had all three sites of reactive astrocytes typically found in the ALS cases: patches of astrocytes, which were especially numerous and occurred in a layered pattern (in LII-III and LV-VI), an increased appearance of reactive astrocytes in the subpial region, and reactive astrocyte processes at the gray/

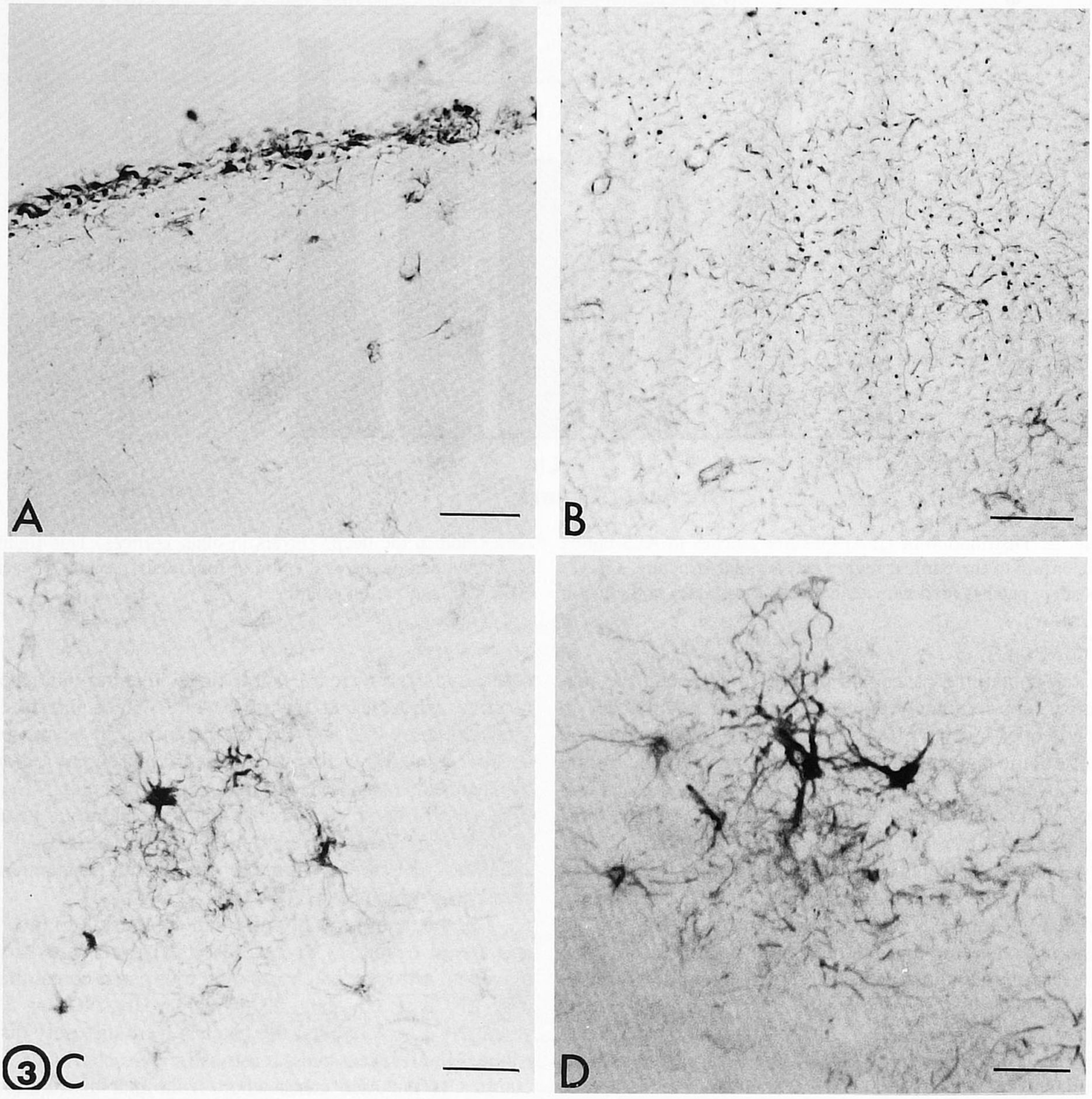

Fig. 3. GFAP immunostaining in neurologically normal and diseased cases. **A:** Gray matter (LII) of a normal control case without reactive astrocytes. **B:** Diffuse gliosis in the gray matter of a control case, C6. **C:** An astrocyte patch in the gray matter of a case of Pick's disease. **D:** A cluster of astrocytes in the gray matter of a case of AD. Bar = 30 μm.

white matter interface (Fig. 3D). These results are summarized in Table I.

β-Amyloid Deposits

Dementia was not apparent in the clinical records of any of the ALS cases. Five of 15 ALS cases (ALS1, ALS2, ALS4, ALS10, and ALS14; average age, 61.6 years), however, had senile plaques in different cortical regions (Table I). These five cases were all of the sporadic form of ALS; neither the familial ALS cases nor the primary lateral sclerosis case had plaques. One of the five was the case of bulbar ALS. In that case (ALS1) and one other case (ALS2, ages 55 and 59 years, respectively) there were both early (Fig. 4A) and classic plaques (Fig. 4B); the other three β-amyloid-positive cases (ALS4, ALS10, and ALS14; ages 63, 67, and 64

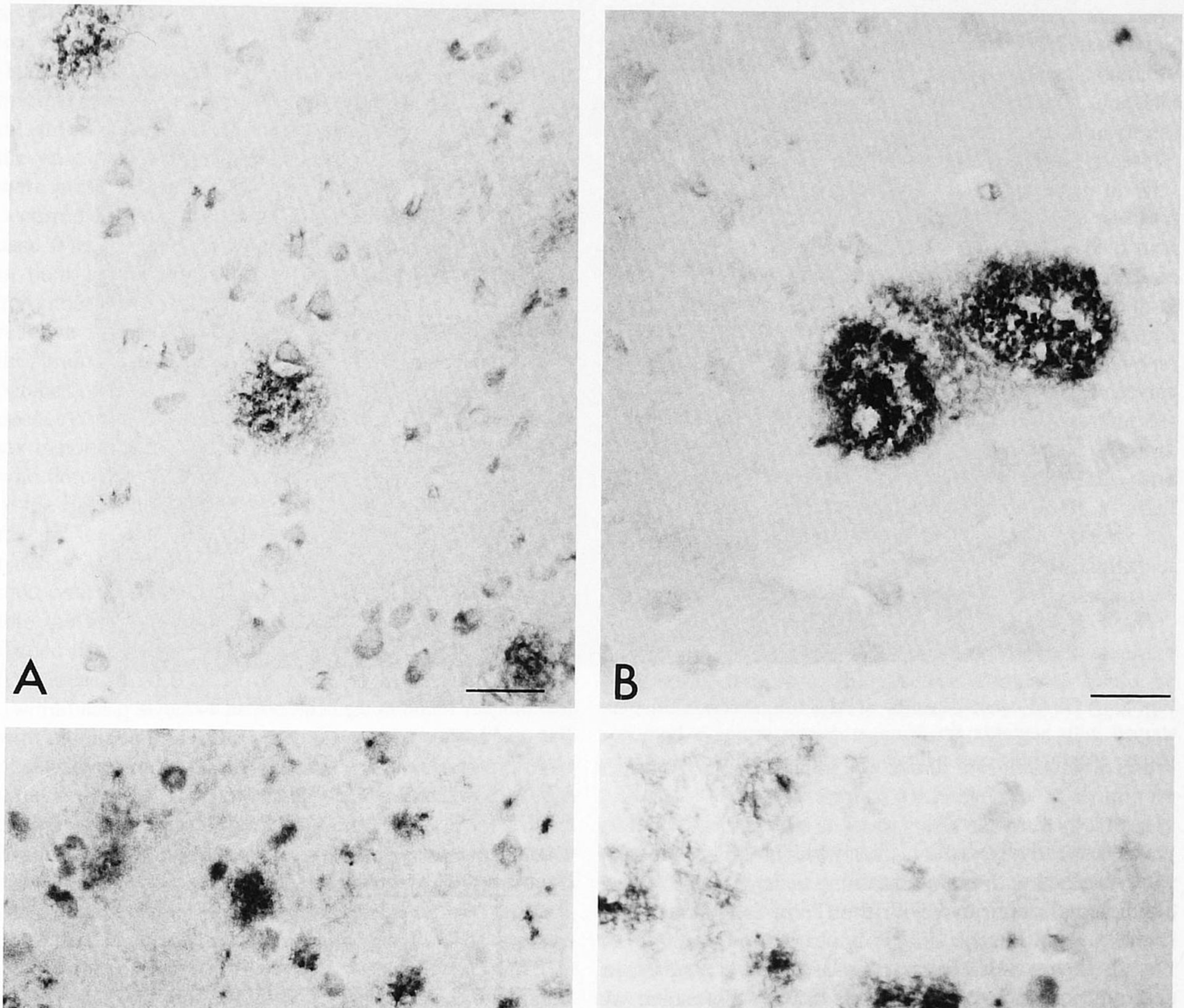

Fig. 4. β-amyloid immunostaining in ALS and AD. **A:** An early plaque in the frontal cortex of ALS. **B:** A classic plaque in ALS cingulate cortex. **C:** An early plaque in the frontal cortex of AD. **D:** A classic plaque in the occipital cortex of AD. These findings was confirmed on near-adjacent sections using modified Bielschowsky silver impregnation. Bar = 30 μm.

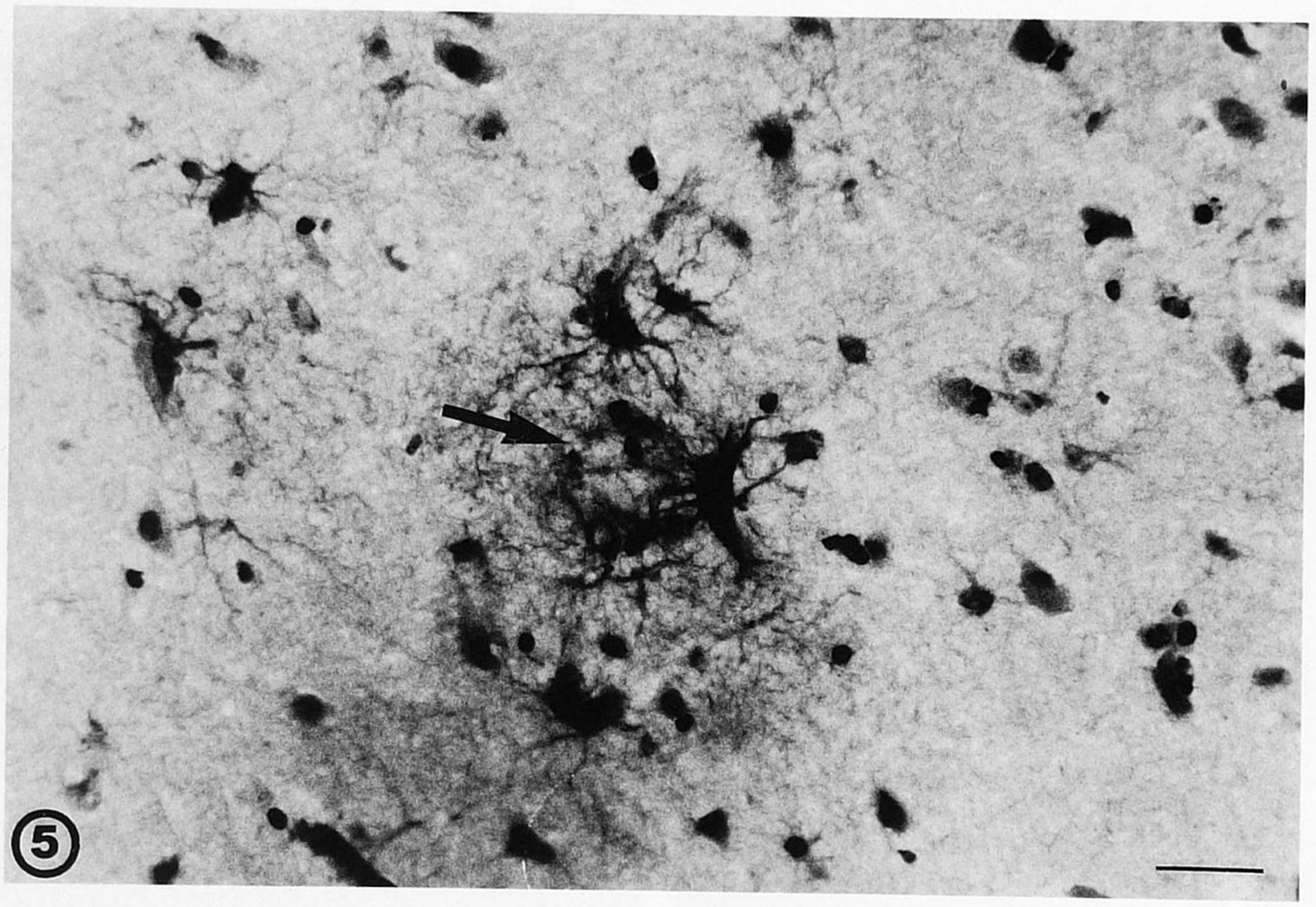

Fig. 5. A GFAP-stained section of ALS frontal cortex counterstained with hematoxylin & eosin demonstrating a homogeneous, eosinophilic core with an appearance similar to an amyloid plaque, found in the center of an astrocyte patch (arrow). Bar = 30 μm.

years, respectively) had only early plaques. These results were obtained with immunostaining using β-amyloid antibodies and confirmed with thioflavin-S and modified Bielschowsky stains.

In the two ALS cases with classic senile plaques, in near-adjacent sections, sometimes the GFAP-positive astrocytes seemed to surround a semi-necrotic core. Hematoxylin and eosin counterstaining of GFAP-stained sections revealed a homogeneous, eosinophilic core with an amyloid-like appearance in the center of the astrocyte patch (Fig. 5). This sort of patch was the exception: the more typical occurrence in ALS was an astrocyte patch without any evidence of blood vessel, senile plaque, or microinfarction. The number of ALS cases with both astrocyte patches and amyloid plaques was four of 15. Thus, there was one ALS case (ALS14) with β-amyloid deposits and no detectable astrocyte patch formation. Table II summarizes the appearance of patches and β-amyloid deposits in ALS.

In the neurologically normal control cases (average age, 65 years ± 12), only one case (C1) displayed β-amyloid deposits, and these were as early plaques. There were no cases with classic plaques. In contrast, among the neurological controls (average age, 73.3 years ± 11.3), five cases (NC1, NC3, NC5, NC6, NC7) had early and/or classic senile plaques. All cases except for NC1 had patches of astrocytes. Both AD cases (average age: 85.5 years) had early and classic plaques (Figs. 4C,D) and patches of reactive astrocytes. These results are found in Table I.

TABLE II. Presence of Astrocyte Patches and β-Amyloid Plaques in ALS According to Age

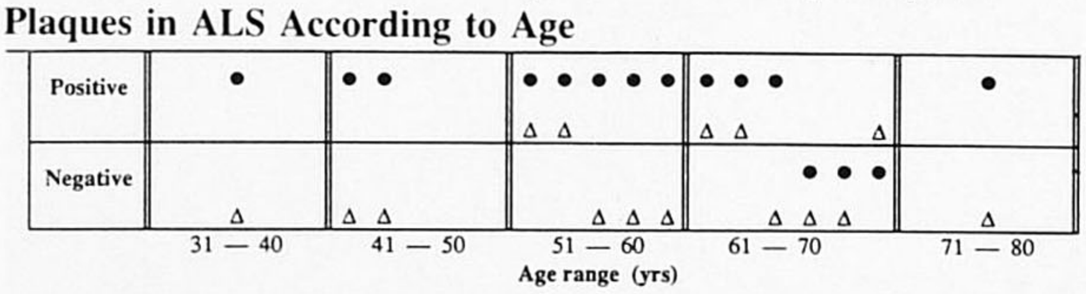

A comparison of GFAP-positive patches (●) and β-amyloid deposits (△) in the 15 ALS cases examined, separated according to age of the patients at death (data from Table I). Astrocyte patches were found in 13/15 cases in all age ranges; cases positive for plaques occurred in 5/15, in the 51–60 and the 61–70 year age ranges. Cases were scored as positive if they had three to five astrocyte patches/section and a minimum of six plaques/section, early and/or classic.

DISCUSSION

This study provides new information about cortical astrocytosis in ALS and gives incentive for further stud-

ies of astrocytes in ALS. Our data indicate that the astrocyte patches described in the motor cortex in ALS (Kamo et al., 1987; Murayama et al., 1991) are present in other cortical areas as well, including frontal, temporal, inferior parietal, cingulate, and occipital cortices. In the cases we analyzed, patches of reactive astrocytes were present in 12 of 15 ALS cases examined. Patches occurred in both familial and sporadic forms of the disease. The patches of astrocytes had an obvious difference in their laminar distribution between the motor cortex and other cortical areas. In the motor cortex, patches of reactive astrocytes were found in the shallow layers of the brain, while in the frontal and temporal cortices patches of reactive astrocytes were more common in the deeper cortical layers. The distribution in the motor cortex is not exactly that found by Murayama et al. (1991), who described increased reactive glia in LIV-V, the site of the Betz cells. Further studies are required to establish the reason for the different laminar distribution of patches in different cortical areas. Astrocytosis in ALS motor cortex at the gray/white matter interface extending into the gray matter (Murayama et al., 1991) was confirmed in our study and was found to exist in other cortical areas in ALS in 11 of 15 cases investigated.

Since patches of astrocytes can occur in association with plaques in AD, the potential overlap of the patches of astrocytes in ALS with plaques was investigated, even though dementia is not usually considered one of the clinical symptoms of ALS (Mulder, 1982; Tandan and Bradley, 1985). In the present study, one-third of the examined ALS cases displayed β-amyloid deposits as early and/or classic plaques. Neither of the two familial cases that we tested had β-amyloid deposits. The average age of the plaque-positive cases was 62 years. In the 51–60 year age range, two of five ALS cases examined had amyloid plaques; in the 61–70 year age range, three of six ALS cases had plaques. This finding, described in Table II, suggests that an increased incidence of plaque formation may occur in ALS. This result is consistent with that of Okamoto et al. (1990), who found a high incidence of plaque formation in ALS, in eight of 21 cases examined. In that study, plaques were present in the 61 year and above age range, while we found plaques even in the 51–60 year age range. For a comparable analysis of non-demented individuals, the prevalence of β-amyloid deposits in the 51–60 year age group was 19% in one study (Davies et al., 1988) and 0% in another (Ogomori et al., 1988); in the 61–70 year age group, it was 30% in the Davies study and 40% in the Ogomori study. In summary, the results of β-amyloid staining show that the incidence of amyloid deposits in ALS may be higher than that of non-demented, age-matched controls.

Because the amyloid deposits are in fewer ALS brain samples than contain astrocyte patches, the amyloid does not appear to cause the patches. These data, however, do not rule out the opposite hypothesis, namely that the patches contribute to amyloid deposits. Our data suggest that this possibility may be best studied in cases, such as ours, that are not end-stage Alzheimer's cases.

One can also ask the more basic question of why reactive astrocytes occur as patches at all. We see two possibilities: either there is a focal insult which in turn causes a reactive astrocyte response in the immediate (circular) vicinity of that insult, or astrocytes of the gray matter receive a signal to undergo cell division, which they do within a circular (or patchy) region. We have no reason to suspect cell replication among the astrocytes within the patch formation, but this is an issue that deserves a direct analysis. As far as a focal insult, we think it quite likely that such an insult does occur in ALS, and we would guess it occurs in the vicinity of a small venule, which, perhaps often, is too small for easy detection. A corollary to this hypothesis is the possibility of a blood-borne insult, which deserves to be evaluated quite carefully in ALS.

ALS commonly occurs in an older than average population; therefore, the reactive astrocytes could be part of an aging process. In an extensive study, Beach et al. (1989) analyzed astrocytes in aged brains using GFAP immunostaining and found an increased astrocytosis in all cases examined (average age at death, 84 years). This increase in astrocytosis occurred as diffusely distributed, individual reactive astrocytes in the cortical gray matter, reactive astrocytes occurring as clusters (or patches) in the upper cortical layers, and a generalized astrocytosis around blood vessels and at the gray/white matter interface. The clusters of reactive astrocytes and the reactive astrocytes at the gray/white matter interface in these very aged specimens are the profile of astrocytosis in ALS. In the aged cases, however, the astrocyte clusters were well correlated with Bielschowsky-positive plaques, while in ALS they are not.

The seven neurologically normal cases (average age, 65 years) in our study had no apparent astrocyte clusters (or patches), but there was a diffuse reactive gliosis in two cases, and another had early plaques. In the seven neurologically diseased cases, where the average age was approximately 10 years older (73 years), four cases contained astrocyte patches and five had early and/or classic amyloid plaques. Neither of our control groups displayed notable astrocytosis at the gray/white matter junction. The patch-containing control cases had a strikingly common feature: all were over 65 years of age, and all had typical classic and early plaques by β-amyloid staining. The average age of our combined control groups (69 years) is approximately one decade younger than the aged cases in the Beach study (Beach et al.,

1989); the ALS brains were from cases two decades younger (average age, 59 years) than those in the Beach study. Thus, ALS brains appear to reveal an astrocytic profile that is similar to that seen in brains from patients two decades older. There are several possible explanations for this observation, one of which could be that there is an early aging process occurring in patients suffering from ALS. This explanation is all the more plausible because of the recent observation that the majority of the cases of familial ALS have a mutation in the gene encoding copper, zinc superoxide dismutase (Rosen et al., 1993). Several of the identified mutations predict a partially active enzyme, which has been demonstrated in familial ALS blood (Deng et al., 1993). A partially active superoxide dismutase could lead to free radical damage and thus a premature aging process in ALS.

The widespread astrocytosis in ALS indicates a more widespread involvement of the brain in ALS, in both familial and sporadic ALS. Other observations supporting the possibility of widespread involvement of the brain in ALS are 1) aberrations of gangliosides in ALS motor, frontal, temporal, and parahippocampal gyri (Rapport et al., 1985), 2) lowered cerebral glucose metabolism that is widespread in brain regions (Dalakas et al., 1987; Hatazawa et al., 1988), 3) reductions of glutamate levels in all CNS areas studied in ALS (Plaitakis et al., 1988), and decreased glutamate transport in the somatosensory cortex, beyond the motor cortex in ALS (Rothstein et al., 1992). Astrogliosis in ALS cortex could be a common response to a variety of insults that actually cause the disease. For instance, beyond the mutations in superoxide dismutase in familial ALS, widespread astrocytosis could be part of an inflammatory response in cases of ALS caused by autoimmunity, for which there is some evidence (e.g., Engelhardt et al., 1989, 1993; Appel et al., 1991; Uchitel et al., 1992). Further experiments should resolve these data and define the roles astrocytes play in ALS.

ACKNOWLEDGMENTS

We acknowledge D.T. Stephenson for preliminary findings of this study. We thank Drs. Dennis Selkoe and Greg.Cole for the generous contribution of antisera. We thank D.T. Stephenson and Dr. F.H. Norris for helpful discussions and editorial comments. This work was supported by the Muscular Dystrophy Association, the Street Foundation, and the ALS and Neuromuscular Research Foundation, San Francisco.

REFERENCES

Appel SH, Engelhardt JI, Garcia J, Stefani E (1991): Immunoglobulins from animal models of motor neuron disease and from human amyotrophic lateral sclerosis patients passively transfer physiological abnormalities to the neuromuscular junction. Proc Natl Acad Sci USA 88:647–651.

Beach TG, Walker R, McGeer EG (1989): Patterns of gliosis in Alzheimer's disease and aging cerebrum. Glia 2:420–436.

Cole G, Masliah E, Huynh TV, DeTeresa R, Terry RD, Okuda C, Saitoh T (1989): An antiserum against amyloid β-protein precursor detects a unique peptide in Alzheimer brain. Neurosci Lett 100:340–346.

Dalakas MC, Hatazawa J, Brooks RA, Chiro GD (1987): Lowered cerebral glucose utilization in amyotrophic lateral sclerosis. Ann Neurol 22:580–586.

Davies L, Wolska B, Hilbich C, Multhaup G, Martins R, Simms G, Beyreuther K, Masters CL (1988): A4 amyloid protein deposition and the diagnosis of Alzheimer's disease: Prelevance in aged brains determined by immunocytochemistry compared with conventional neuropathologic techniques. Neurology 38: 1688–1693.

Davison C (1941): Amyotrophic lateral sclerosis. Origin and extent of the upper motor neuron lesion. Arch Neurol Psychiatry 46: 1039–1056.

Deng H-X, Hentati A, Tainer JA, Iqbal Z, et al. (1993): Amyotrophic lateral sclerosis and structural defects in Cu,Zn superoxide dismutase. Science 261:1047–1051.

Engelhardt JI, Appel SH, Killian JM (1989): Experimental autoimmune motoneuron disease. Ann Neurol 26:368–376.

Engelhardt JI, Tajti J, Appel SH (1993): Lymphocytic infiltrates in the spinal cord in amyotrophic lateral sclerosis. Arch Neurol 50: 30–36.

Hammer RP, Tomiyashu U, Scheibel AB (1979): Degeneration of human Betz cell due to amyotrophic lateral sclerosis. Exp Neurol 63:336–346.

Harpin ML, Delaere P, Javoy-Agid F, Bock E, Jacque C, Delpech B, Villarroya H, Duyckaerts C, Hauw JJ, Baumann N (1990): Glial fibrillary acidic protein and βA4 protein deposits in temporal lobe of aging brain and senile dementia of the Alzheimer type: Relation with the cognitive state and with quantitative studies of senile plaques and neurofibrillary tangles. J Neurosci Res 27:587–594.

Hatazawa J, Brooks RA, Dalakas MC, Mansi L, Chiro GD (1988): Cortical motor-sensory hypometabolism in amyotrophic lateral sclerosis: A PET study. J Comput Assist Tomogr 12:630–636.

Hirano A (1991): Cytopathology of amyotrophic lateral sclerosis. In Rowland LA (ed): "Amyotrophic Lateral Sclerosis and Other Motor Neuron Diseases." New York: Raven Press, pp 91–101.

Horoupian DS, Thal L, Katzman R, Terry RD, Davies P, Hirano A, DeTerasa R, Fuld PA, Petito C, Blass J, Ellis JM (1984): Dementia and motor neuron disease: Morphometric, biochemical and Golgi studies. Ann Neurol 16:305–313.

Iwasaki Y, Kinoshita M, Ikeda K, Takamiya K, Shiojima T (1990): Cognitive impairment in amyotrophic lateral sclerosis and its relation to motor disabilities. Acta Neurol Scand 81:141–143.

Joachim CL, Mori H, Selkoe D (1989): Amyloid β-protein deposition in tissues other than brain in Alzheimer's disease. Nature 341: 226–230.

Kamo H, Haebara H, Akiguchi I, Kameyama M, Kimura H, McGeer PL (1987): A distinctive distribution of reactive astroglia in the precentral cortex in amyotrophic lateral sclerosis. Acta Neuropathol (Berl) 74:33–38.

Kitamoto T, Ogomori K, Tateishi J, Prusiner SB (1987): Methods in laboratory investigation. Formic acid pretreatment enhances immunostaining of cerebral and systemic amyloids. Lab Invest 57:230–236.

Kushner PD, Stephenson DT, Wright S, Cole GM, Greco CM (1989)

Monoclonal antibody Tor 23 binds a subset of neural cells in the human cortex and displays an altered binding distribution in Alzheimer's disease. J Neuropathol Exp Neurol 48:692–708.

Kushner PD, Stephenson DT, Wright S (1991): Reactive astrogliosis is widespread in the subcortical white matter of amyotrophic lateral sclerosis brain. J Neuropathol Exp Neurol 50:263–277.

Lawyer T, Netsky MG (1953): Amyotrophic lateral sclerosis: A clinicoanatomic study of 53 cases. Arch Neurol Psychiatry 69:171–192.

Mitsuyama Y, Takamiya S (1979): Presenile dementia with motor neuron disease in Japan: A new entity? Arch Neurol 36:592–593.

Mulder DW (1982): Clinical limits of amyotrophic lateral sclerosis. In Rowland LP (ed): ''Human Motor Neuron Diseases.'' New York: Raven Press, pp 15–22.

Murayama S, Inoue K, Kawakami H, Bouldin TW, Suzuki K (1991): A unique pattern of astrocytosis in the primary motor area in amyotrophic lateral sclerosis. Acta Neuropathol 82:456–461.

Myrianthopoulos NC, Smith JK (1962): Amyotrophic lateral sclerosis with progressive dementia. Neurology 12:603–610.

Ogomori K, Kitamoto T, Tateishi J, Sato Y, Tashima T (1988): Aging and cerebral amyloid: Early detection of amyloid in the human brain using biochemical extraction and immunostain. J Gerontol Bio Sci 43:B157–162.

Okamoto K, Shoji M, Harigaya Y, Yanagisawa T, Hirai S (1990): Senile changes in amyotrophic lateral sclerosis. Igaku no Ayumi (Progress in Medicine) 152:127–128.

Plaitakis A, Constantakakis E, Smith J (1988): The neuroexcitotoxic amino acids glutamate and aspartate are altered in the spinal cord and brain in amyotrophic lateral sclerosis. Ann Neurol 24:446–449.

Rapport MM, Donnenfeld H, Brunner W, Hungund B, Bartfeld H (1985): Ganglioside patterns in amyotrophic lateral sclerosis brain regions. Ann Neurol 18:60–67.

Rodgers-Johnson P, Garruto RM, Yanagihara R, Chen KM, Gajdusek DC, Gibbs CJ (1986): Amyotrophic lateral sclerosis and parkinsonism-dementia on Guam: A 30-year evaluation of clinical and neuropathologic trends. Neurology 36:7–13.

Rosen DR, Siddique T, Patterson D, Figlewicz DA, et al. (1993). Mutations in the Cu/Zn superoxide dismutase gene are associated with familial amyotrophic lateral sclerosis. Nature 362: 59–62.

Rothstein JD, Martin LJ, Kuncl RW (1992): Decreased glutamate transport by the brain and spinal cord in amyotrophic lateral sclerosis. N Engl J Med 326:1464–1468.

Rowland LP (1991): Ten central themes in a decade of ALS research. In Rowland LP (ed): ''Amyotrophic Lateral Sclerosis and Other Motor Neuron Diseases.'' New York: Raven Press, pp 3–23.

Rozemuller JM, Eikelenboom P, Stam FC, Beyreuther K, Masters CL (1989): A4 protein in Alzheimer's disease: Primary and secondary cellular events in extracellular amyloid deposition. J Neuropathol Exp Neurol 48:674–691.

Shimada A, Kuwamura M, Umemura T, Takada K, Ohama E, Itakura C (1991): Modified Bielschowsky and immunohistochemical studies on senile plaques in aged dogs. Neurosci Lett 129:25–28.

Tandan R, Bradley WG (1985): Amyotrophic lateral sclerosis: Part 1. Clinical features, pathology, and ethical issues in management. Ann Neurol 18:271–280.

Uchitel OD, Scornik F, Protti DA, Fumberg CG, Alvarez V, Appel SH (1992): Long-term neuromuscular dysfunction produced by passive transfer of amyotrophic lateral sclerosis immunoglobulins. Neurology 42:2175–2180.

Wikstrom J, Paetau A, Palo J, Sulkava R, Haltia M (1982): Classic amyotrophic lateral sclerosis with dementia. Arch Neurol 39: 681–683.

Journal of Neuroscience Research 38:348–357 (1994)

Subcellular Localization of the F5 Protein to the Neuronal Membrane-Associated Cytoskeleton

M. Arai and J.A. Cohen
Department of Neurology, University of Pennsylvania School of Medicine, Philadelphia

F5 was identified originally as an interleukin-2-regulated gene in the murine helper T-lymphocyte clone L2. Subsequent studies demonstrated high levels of F5 mRNA and protein in mature neurons in adult mouse central and peripheral nervous systems. The F5 protein was present in dendrites and perikarya but not in axons. In the present studies, the intracellular localization of the F5 protein in adult mouse brain was determined by subcellular fractionation and Western blotting. Although the deduced F5 sequence predicts a soluble protein, virtually no F5 immunoreactivity was found in the cytosol. The F5 protein was restricted to the P2 crude mitochondrial and P3 crude microsomal particulate fractions. Within the P2 fraction, F5 protein was enriched in the P2B synaptosomal subfraction. The results of temperature-dependent phase separation with Triton X-114 and alkaline extraction with sodium carbonate of the P2 and P3 fractions were consistent with the F5 protein being an extrinsic membrane-associated protein. Although essentially all of the F5 protein in the P3 fraction was membrane-associated, a substantial proportion of P2-associated F5 protein and nearly all of the synaptosomal F5 protein was detergent-insoluble. Direct isolation and subfractionation of brain cytoskeleton confirmed colocalization of F5 immunoreactivity with the membrane-associated cytoskeleton and postsynaptic densities. These studies suggest that the F5 protein, which has a large number of potential phosphorylation sites, plays a role in membrane-cytoskeletal interactions and in dynamic aspects of synaptic structure or function. © 1994 Wiley-Liss, Inc.

Key words: subcellular fractionation, neuron, cytoskeleton, postsynaptic densities

INTRODUCTION

F5 was identified originally by differential hybridization cDNA library screening as an interleukin-2-regulated gene in L2 cells, a murine helper T-lymphocyte clone (Sabath et al., 1990). Northern blot analyses demonstrated that the F5 mRNA was expressed at low levels in lymphoid tissues and at a high level in the nervous system of adult mouse but not in other tissues (Cohen et al., 1992). In situ hybridization histochemistry (ISHH) studies demonstrated widespread expression of F5 mRNA by neurons in the brain, peripheral nervous system, and neuroretina and by choroid plexus epithelial cells (Arai et al., 1992). Neuronal expression of F5 mRNA exhibited two interesting features. First, the level of expression appeared to correlate with the size of the neuronal perikarya, the extent of dendritic arborization, or the length of the axonal projection. Neurons in layer V of neocortex, cerebellar Purkinje cells, pyramidal cells in the hippocampus, the granule cell layer in the dentate gyrus, and large motor neurons in the brain stem and anterior horn of the spinal cord exhibited the highest levels of F5 mRNA expression. Second, expression of F5 mRNA was a feature of the mature neuronal phenotype. On Northern blot studies, F5 mRNA was undetectable or expressed at a very low level in cerebrum up to postnatal day 14 and progressively increased to a maximum 56 days after birth (Cohen et al., 1992) (J.A. Cohen and S.S. Scherer, unpublished data). Induction of F5 gene expression coincided temporally and spatially with synaptogenesis (Arai et al., 1992; Cohen et al., 1992). Neuronal expression in dorsal root ganglia rapidly decreased following axotomy (J.A. Cohen and S.S. Scherer, unpublished data). Thus, in the nervous system expression of F5 is a novel, specific marker for mature neurons.

Received July 29, 1993; revised and accepted December 1, 1993.

Address reprint requests to Dr. Jeffrey A. Cohen, Department of Neurology, Hospital of the University of Pennsylvania, 3400 Spruce Street, Philadelphia, PA 19104-4283.

M. Arai is now at Department of Neurology, Takeda General Hospital, Aizu-Wakamatsu City, Japan.

Abbreviations used: ConA, concanavalin A; NF-M, medium-sized neurofilament subunit; PMSF, phenylmethylsulfonyl fluoride; PSDs, postsynaptic densities; SDS-PAGE, sodium dodecyl sulfate-polyacrylamide gel electrophoresis; TBS, Tris-buffered saline.

Sequence analysis of a full-length F5 cDNA clone isolated from adult mouse brain demonstrated an open reading frame of 1,125 bp encoding a 42-kDa basic protein (Cohen et al., 1992). Although the putative F5 coding region showed substantial cross-species hybridization, the deduced F5 protein had no similarity to previously reported sequences and no features suggesting its intracellular localization or function. The most striking structural feature was the presence of a large number of potential phosphorylation sites for a variety of protein kinases, suggesting that the function of the F5 protein is regulated by its phosphorylation state or that it is a component of a signal transduction pathway.

We previously described the generation of polyclonal rabbit anti-F5 antibody (Arai and Cohen, 1993). Immunohistochemical studies of adult mouse brain using this antibody demonstrated F5 immunoreactivity in neuronal perikarya and dendrites but not axons. The neurons expressing the highest levels of F5 protein corresponded to those with the highest levels of F5 mRNA. Choroid plexus epithelial cells also exhibited strong reactivity, which was localized to their basal aspect. In the present studies, the subcellular localization of the F5 protein in adult mouse brain was determined.

MATERIALS AND METHODS

Western Blotting

Sodium dodecyl sulfate-polyacrylamide gel electrophoresis (SDS-PAGE) and Western blotting were performed exactly as previously described (Arai and Cohen, 1993). Samples containing 5, 10, or 20 μg protein were fractionated on 7.5, 10, or 12% polyacrylamide gels containing 0.1% SDS. Primary antibodies included affinity-purified polyclonal rabbit anti-F5 antibody (Arai and Cohen, 1993), mouse monoclonal anti-middle-sized neurofilament subunit (NF-M) antibody RMO108 (Lee et al., 1987), mouse monoclonal anti-β-tubulin antibody KMX-1 (Boehringer-Mannheim, Indianapolis, IN), and mouse monoclonal anti-pan-actin antibody C4 (Boehringer-Mannheim). Alkaline phosphatase-conjugated goat antibodies (Boehringer-Mannheim) of the appropriate species specificities were used as secondary antibodies. Glycoproteins were stained with digoxigenin-labeled concanavalin A (ConA) and alkaline phosphatase-conjugated anti-digoxigenin antibody (both from Boehringer-Mannheim). Signal intensity was quantified by computer-assisted video densitometry.

Subcellular Fractionation

Subcellular fractionation of adult mouse brain was carried out by differential centrifugation according to the method of Gray and Whittaker (1962). Mice were deeply anesthetized with CO_2. The brains were removed and the cerebral hemispheres were dissected. Specimens were kept on ice and used immediately or stored at −80°C. The brains were homogenized in a solution containing 0.32 M sucrose; 5 mM Tris-HCl, pH 7.5; and 1 mM phenylmethylsulfonyl fluoride (PMSF). The homogenate was centrifuged at $1{,}000g_{av}$ for 5 min yielding the crude nuclear pellet (P1) and supernatant 1 (S1). S1 was centrifuged at $12{,}500g_{av}$ for 15 min yielding the crude mitochondrial pellet (P2) and supernatant 2 (S2). S2 was centrifuged at $100{,}000g_{av}$ for 45 min yielding the crude microsomal pellet (P3) and the cytosolic fraction (S3). P3 was washed in a solution containing 0.5 M KCl and 150 mM Tris-HCl, pH 8.0, prior to SDS-PAGE and Western blotting with anti-F5 antibody.

The P2 fraction was subfractionated by the method of Gurd et al. (1974) as modified by Krueger et al. (1977). The P2 pellet was resuspended in 14% Ficoll (wt/vol) in 0.32 M sucrose. A discontinuous Ficoll density gradient was formed by overlaying the P2 suspension with 7.5% Ficoll in 0.32 M sucrose and then with 0.32 M sucrose. The gradient was centrifuged at $92{,}000g_{av}$ for 2 hr in a Sorvall (Wilmington, DE) TH-641 swinging bucket rotor. The myelin fraction (P2A) was collected at the 0–7.5% Ficoll interface. The synaptosomal fraction (P2B) was collected at the 7.5–14% Ficoll interface. The pellet represented the purified mitochondrial fraction (P2C). All three fractions were washed in 0.32 M sucrose prior to analysis by SDS-PAGE and Western blotting with anti-F5 antibody.

Sodium Pyrophosphate Treatment

Aliquots of brain fractions containing 200 μg protein were treated at 4°C for 20 min with 15 mM sodium pyrophosphate, pH 8.2, in 0.25 M sucrose (Amar-Costesec et al., 1974). Soluble and insoluble materials were separated by centrifugation at $16{,}000g_{av}$ for 20 min. Insoluble pellets were washed with 10 mM Tris-buffered saline (TBS; 10 mM Tris-HCl, pH 7.5, and 150 mM NaCl) prior to analysis by SDS-PAGE and Western blotting with anti-F5 antibody.

Temperature-Induced Phase Separation With Triton X-114

Temperature-induced phase partitioning was carried out by the method of Bordier (1981) with minor modifications. Triton X-114 (Sigma, St. Louis, MO) was precondensed three times. Aliquots of P2 and P3 fractions containing 100 μg protein were solubilized in 1% Triton X-114 (vol/vol) in 10 mM TBS at 0°C for 30 min at a detergent to protein ratio of 100:1 then centrifuged at $16{,}000g_{av}$ for 20 min. The Triton X-114-soluble material was phase partitioned at 30°C. The aqueous phase was reextracted twice with 0.5% Triton X-114 and the detergent phase was washed twice with 10 mM TBS.

Protein in the aqueous and detergent phases was precipitated with 0.4 M trichloroacetic acid, washed twice with diethylether/ethanol (1:1 vol/vol), and dissolved in SDS sample buffer for analysis by SDS-PAGE and Western blotting with anti-F5 antibody.

Alkaline Extraction

Alkaline extraction was carried out by the method of Fujiki et al. (1982). Aliquots of the P2 and P3 fractions containing 200 μg protein were incubated in 1 ml of 0.1 M sodium carbonate, pH 11.5, at 4°C for 30 min and then centrifuged at $16,000g_{av}$ for 20 min. Protein in the supernatant was precipitated with 0.4 M trichloroacetic acid and washed with diethylether/ethanol (1:1 vol/vol). The sodium carbonate-insoluble pellet and the material precipitated from the supernatant were dissolved in SDS sample buffer and analyzed by SDS-PAGE and Western blotting with anti-F5 antibody.

Triton X-100 Extraction of Subcellular Fractions

Aliquots of brain fractions containing 200 μg protein were extracted twice with 2% Triton X-100 (vol/vol) in 10 mM TBS at a detergent to protein ratio of 100:1 at 4°C for 20 min. Soluble and insoluble materials were separated by centrifugation at $16,000g_{av}$ for 20 min. Insoluble pellets were washed with 10 mM TBS and analyzed by SDS-PAGE and Western blotting with anti-F5 antibody.

Isolation and Subfractionation of Brain Cytoskeleton

Cytoskeleton was isolated from adult mouse brain and subfractionated by the method of Moss (1983) with minor modifications. Briefly, mouse brains were homogenized in 2% Triton X-100 (vol/vol) in Tris/$MgCl_2$ buffer (10 mM Tris-HCl, pH 7.5; 2 mM $MgCl_2$; and 1 mM PMSF) at a detergent to protein ratio of 5:1. The homogenate was centrifuged at $100,000g_{av}$ for 30 min. The detergent-insoluble pellet was homogenized in 10% sucrose (wt/vol) in Tris/$MgCl_2$ buffer. A discontinuous sucrose gradient consisting of 50% and 30% sucrose layers in Tris/$MgCl_2$ buffer was overlayed with the detergent-insoluble material suspended in 10% sucrose in Tris/$MgCl_2$ buffer and centrifuged at $100,000g_{av}$ for 3 hr in a Sorvall TH-641 swinging bucket rotor. Fractions were collected from the sucrose steps and the interfaces and washed in 10 mM TBS. Aliquots of each fraction containing 20 μg protein were analyzed by SDS-PAGE and Western blotting with antibodies reactive with F5, NF-M, β-tubulin, or pan-actin.

Isolation of Postsynaptic Densities (PSDs)

The PSD fraction was prepared by the method of Cohen et al. (1977). Briefly, the P2B synaptosomal fraction was treated with 0.5% Triton X-100, and the detergent-insoluble material collected by centrifugation at $200,000g_{av}$ for 2 hr on a discontinuous sucrose density gradient. The material at the 1.5–2.0 M sucrose interface was collected and washed in a solution containing 0.5% Triton X-100; 75 mM KCl; and 3 mM Tris-HCl, pH 8.0. Purified PSDs were analyzed by SDS-PAGE and Western blotting with digoxigenin-conjugated ConA or anti-F5 antibody.

RESULTS

Subcellular Distribution of F5 Immunoreactivity in Adult Mouse Brain

The deduced sequence of the F5 protein predicted a hydrophilic protein but provided no indication of its subcellular localization (Cohen et al., 1992). Recombinant F5 protein synthesized by in vitro translation or in *Escherichia coli* was freely soluble (Arai and Cohen, 1993). These observations plus the lack of protein motifs necessary for targeting to membranes or to the nucleus suggested that the F5 protein is a soluble, cytoplasmic protein. To confirm the subcellular localization of the F5 protein in adult mouse brain, fractionation studies were carried out by a standard method (Gray and Whittaker, 1962) followed by SDS-PAGE and Western blotting with anti-F5 antibody (Fig. 1). Surprisingly, essentially no F5 immunoreactivity was detected in the S3 cytosolic fraction. Rather, F5 reactivity in brain was restricted to the particulate fractions. The crude mitochondrial fraction (P2), which contains mitochondria, myelin and plasma membrane, and synaptosomes (Gray and Whittaker, 1962), showed the highest level of F5 immunoreactivity. The crude microsomal fraction (P3), which contains rough and smooth endoplasmic reticulum, Golgi, and plasma and outer mitochondrial membranes (Gray and Whittaker, 1962), demonstrated moderate immunoreactivity. The P1 fraction, which contains neuronal and glial nuclei and cellular debris (Gray and Whittaker, 1962), demonstrated a very low level of F5 reactivity. When purified nuclei (Thompson, 1973) were analyzed, essentially no reactivity was seen (data not shown), suggesting that the modest reactivity in P1 resulted from contamination.

The P2 crude mitochondrial fraction was further subfractionated by ultracentrifugation on a discontinuous Ficoll density gradient (Krueger et al., 1977; Gurd et al., 1982) and analyzed by Western blotting with anti-F5 antibody (Fig. 2). F5 immunoreactivity was greatly enriched in the P2B synaptosomal fraction, which contains both pre- and postsynaptic membrane elements (Gurd et al., 1982). The P2A fraction, which is enriched in myelin and other plasma membranes (Gurd et al., 1982), contained moderate F5 immunoreactivity. P2C, the mi-

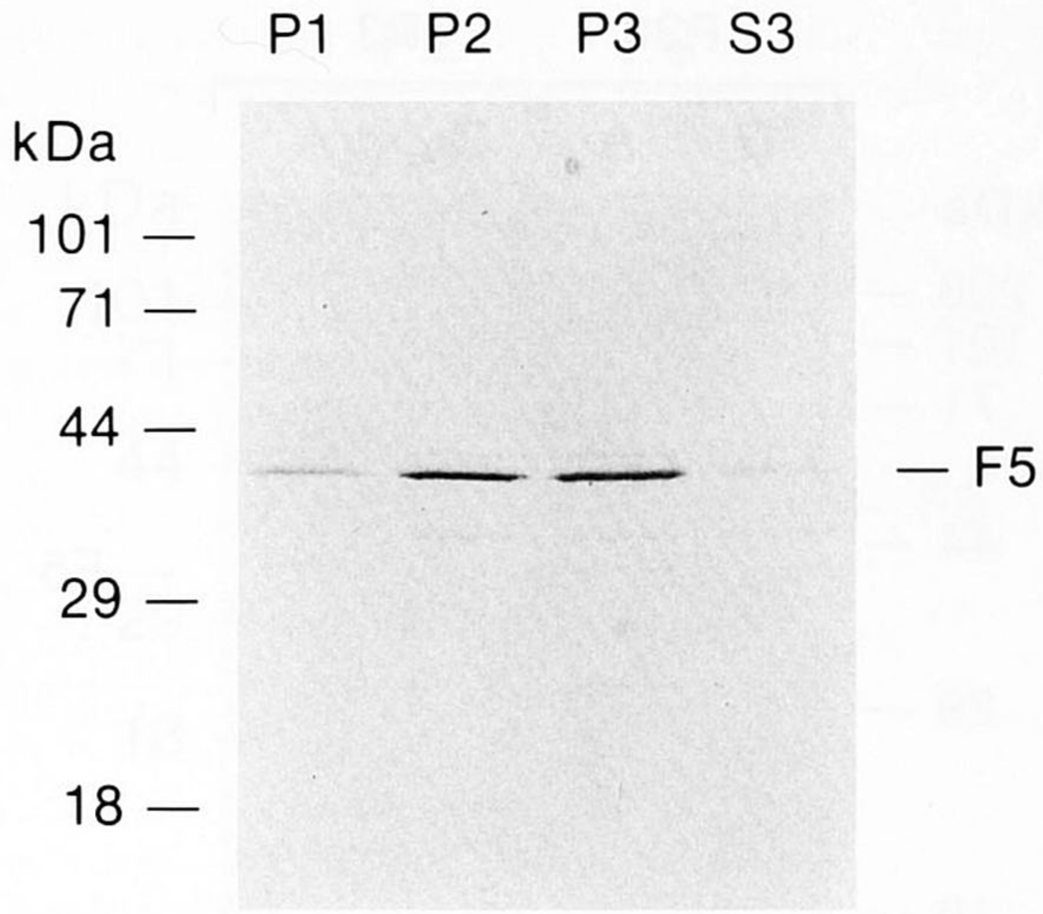

Fig. 1. Subcellular distribution of F5 immunoreactivity in adult mouse brain. Homogenate of adult mouse cerebral hemisphere was fractionated by differential centrifugation (Gray and Whittaker, 1962). Aliquots containing 10 μg protein of the crude nuclear (P1), crude mitochondrial (P2), crude microsomal (P3), and cytosolic (S3) fractions were analyzed by SDS-PAGE and Western blotting with anti-F5 antibody. Although F5 is a hydrophilic protein, F5 immunoreactivity was detected in the particulate P2 and P3 fractions.

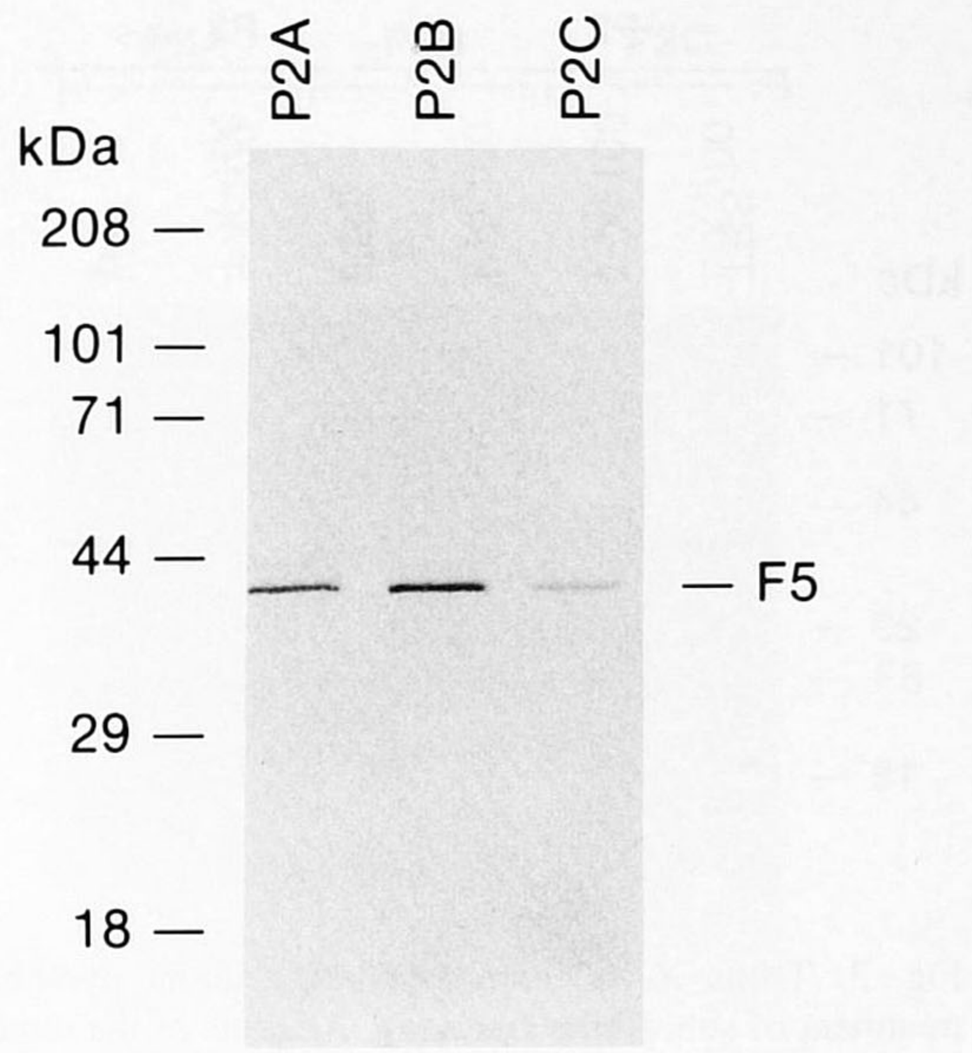

Fig. 2. Subfractionation of the P2 fraction. The P2 crude mitochondrial fraction of adult mouse brain was centrifuged on a discontinuous Ficoll gradient, yielding the myelin (P2A), synaptosomal (P2B), and mitochondrial (P2C) subfractions. Aliquots containing 10 μg protein were analyzed by SDS-PAGE and Western blotting with anti-F5 antibody. F5 immunoreactivity was greatly enriched in the P2B synaptosomal subfraction. Lower levels were detected in the myelin and mitochondrial subfractions.

tochondria-containing pellet (Gurd et al., 1982), demonstrated a very low level of reactivity. The concentration of F5 protein in the P2A was 68% of that in the P2B subfraction, and P2C was 22%.

Previous Western blot studies of adult mouse brain homogenate demonstrated two F5 protein bands, a predominant 42-kDa form and a minor 39-kDa form (Arai and Cohen, 1993). Although both forms were detected in Western blots of subcellular fractions (Figs. 1, 2), the 39-kDa band typically was very faint. There were no systematic differences in the subcellular distributions of the two forms. Thus, the functional significance of the existence of two F5 protein forms remains unclear and does not appear to play a role in intracellular trafficking.

Characterization of the Membrane-F5 Protein Interaction

The predicted F5 protein has a net isoelectric point (pI) of 9.3 (Cohen et al., 1992). Nonequilibrium pH gradient electrophoresis (O'Farrell, 1975; O'Farrell et al., 1977) followed by Western blotting demonstrated that the F5 protein in adult mouse brain and subcellular fractions had pI of 8.3, confirming that it is a basic protein (M. Arai and J.A. Cohen, unpublished data). Previous studies have shown that the P3 microsomal fraction can be contaminated by ionic adsorption of basic proteins onto ribosomes (Scheele et al., 1978). Thus, it was conceivable that the F5 protein associated nonspecifically with components of the particulate fractions during homogenization. To test this possibility, the P2 and P3 fractions were treated with 15 mM sodium pyrophosphate, pH 8.2, which has been reported to disrupt nonspecific ionic interactions of basic proteins with membrane fractions (Amar-Costesec et al., 1974), and then analyzed by SDS-PAGE and Western blotting. The amount of the F5 protein in either the P2 or the P3 fraction did not change appreciably after this treatment (Fig. 3), which argues against nonspecific contamination with F5 protein during subcellular fractionation.

To characterize the interaction of F5 protein with membrane components of the P2 and P3 fractions, temperature-dependent phase separation studies with Triton X-114 (Bordier, 1981) were carried out. F5 immunoreactivity was found exclusively in the aqueous phases derived from both the P2 and P3 fractions (Fig. 4), suggesting that the F5 protein is a hydrophilic, peripheral membrane protein. Some amphipathic integral membrane proteins such as the acetylcholine receptor have been found anomalously in the aqueous phase after temperature-dependent phase partitioning with Triton X-114 (Maher and Singer, 1985). To rule out similar behavior by the F5 protein, aliquots of the P2 and P3 fractions were treated with 0.1 M sodium carbonate, pH 11.5,

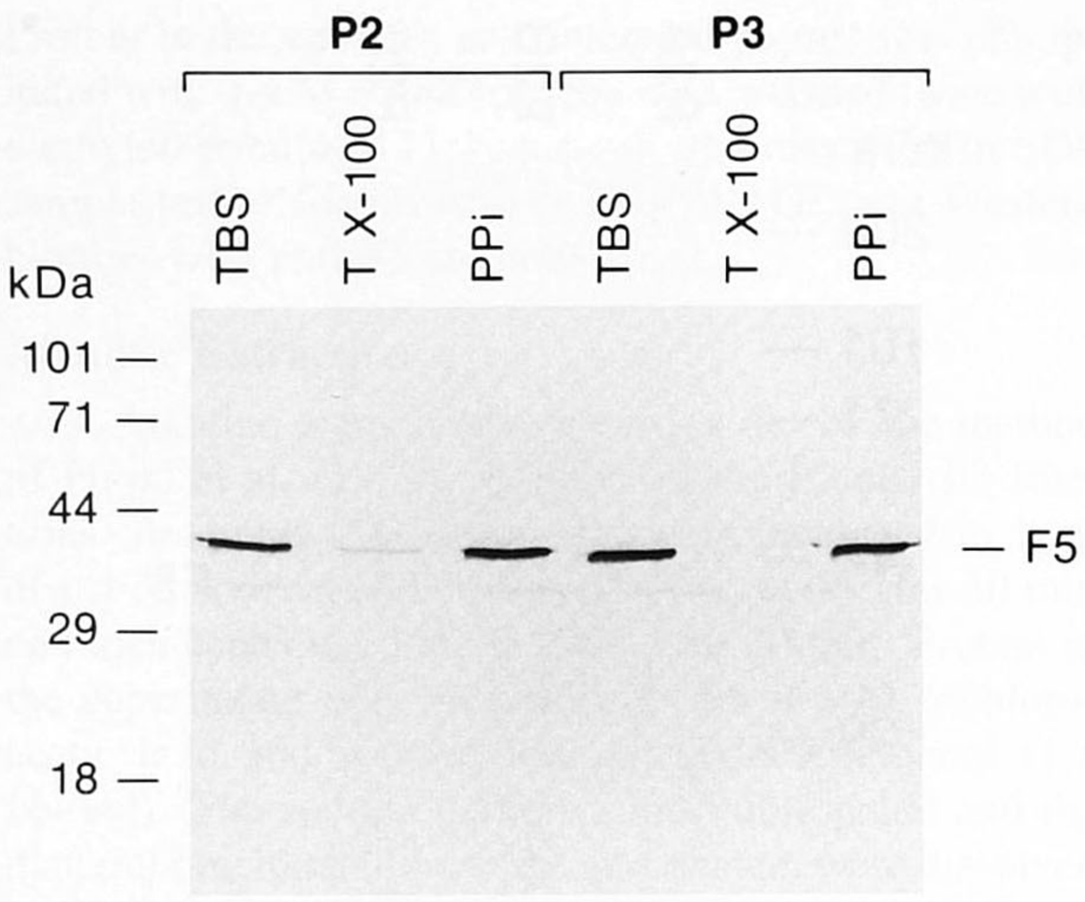

Fig. 3. Triton X-100 extraction and sodium pyrophosphate treatment of subcellular fractions. Aliquots of the crude mitochondrial (P2) and microsomal (P3) fractions containing 200 μg protein were treated either with 2% Triton X-100 (TX-100) at a detergent to protein ratio of 100:1 or with 15 mM sodium pyrophosphate (PPi). Incubation of each fraction in 50 mM TBS (TBS) served as a negative control. After centrifugation, insoluble pellets were dissolved in 200 μl SDS sample buffer, and a 20-μl aliquot of each sample was analyzed by SDS-PAGE and Western blotting with anti-F5 antibody. Sodium pyrophosphate treatment, which disrupts nonspecific ionic interactions of basic proteins with membrane, did not remove F5 immunoreactivity from the P2 or P3 fractions. While essentially 100% of the P3-associated F5 immunoreactivity was removed by nonionic detergent extraction, 20% of the P2-associated F5 immunoreactivity was detergent-insoluble.

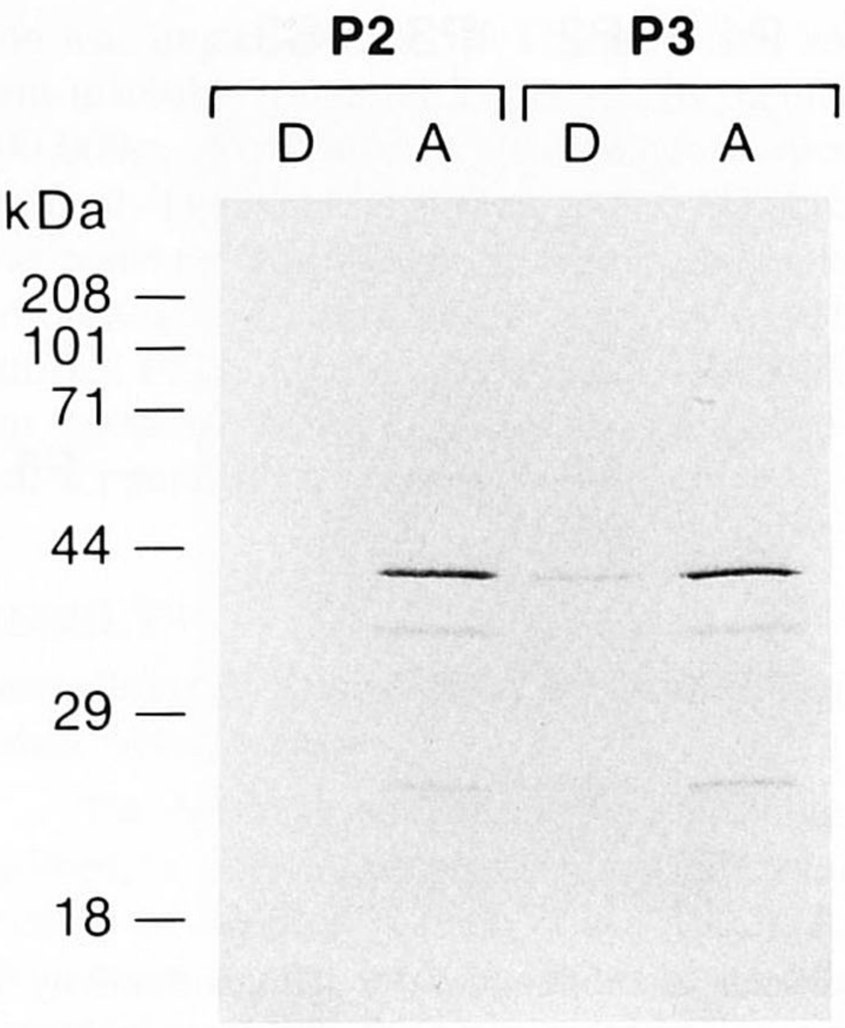

Fig. 4. Temperature-dependent phase partitioning of F5 immunoreactivity. The crude mitochondrial (P2) and microsomal (P3) fractions containing 200 μg protein were extracted with 2% Triton X-114 at 4°C. Triton X-114-soluble proteins were phase separated at 30°C. Proteins partitioned to detergent (D) and aqueous (A) phases were precipitated with trichloroacetic acid and washed with ethanol/ethyl ether (1:1 vol/vol). Aliquots containing approximately 20 μg protein were analyzed by SDS-PAGE and Western blotting with anti-F5 antibody. All of the F5 protein in the P2 fraction and virtually all in the P3 fraction partitioned to the aqueous phase.

which would be expected to release extrinsic membrane-associated proteins only (Fujiki et al., 1982). F5 immunoreactivity was removed completely by alkaline extraction (Fig. 5), further confirming that the F5 protein is loosely associated with and likely to be peripheral to the membrane components of both the P2 and P3 fractions.

Association of F5 Protein With Brain Cytoskeleton

In addition to membranous material, the particulate fractions contain cytoskeletal elements. To determine with which the F5 immunoreactivity in adult mouse brain was associated, the P3 fraction, P2 fraction, and P2 subfractions were extracted twice with Triton X-100 at a high detergent to protein ratio of 100:1. Less than 5% of the F5 immunoreactivity in the P3 fraction remained in the detergent-insoluble pellet, suggesting that most of the F5 protein in the P3 fraction is membrane-associated. Approximately 20% of the F5 immunoreactivity in the P2 fraction remained in the detergent-insoluble pellet (Fig. 3). The F5 protein in the P2A and P2B subfractions was detergent-insoluble; essentially no immunoreactivity was removed by detergent extraction (Fig. 6). In contrast, most of the F5 protein in the P2C subfraction was soluble in nonionic detergent; only 12% of the F5 protein in the P2C subfraction was retained in the insoluble pellet. Since the P2C mitochondrial subfraction comprised 75% of the total P2 protein, it is likely that the F5 immunoreactivity found at low concentration in this subfraction accounted for most of the detergent-soluble F5 protein in the P2 fraction. The bulk of the detergent-insoluble F5 immunoreactivity in the P2 fraction probably was found in the P2A myelin-plasma membrane subfraction, which contained 12% of the P2 protein, and P2B synaptosomal subfraction, which contained 13% of the P2 protein.

The detergent-insolubility of the F5 protein in the P2A and P2B subfractions suggested association with cytoskeletal elements. To confirm this association, cytoskeleton was isolated from adult mouse brain homogenate and fractionated by discontinuous sucrose gradient centrifugation (Moss, 1983). By this method, membrane-associated cytoskeleton is enriched in the 10/30% interface fraction. The 50% sucrose step contains predominantly cytoplasmic cytoskeleton. The 30/50% interface contains a mixture of the two cytoskeletal fractions.

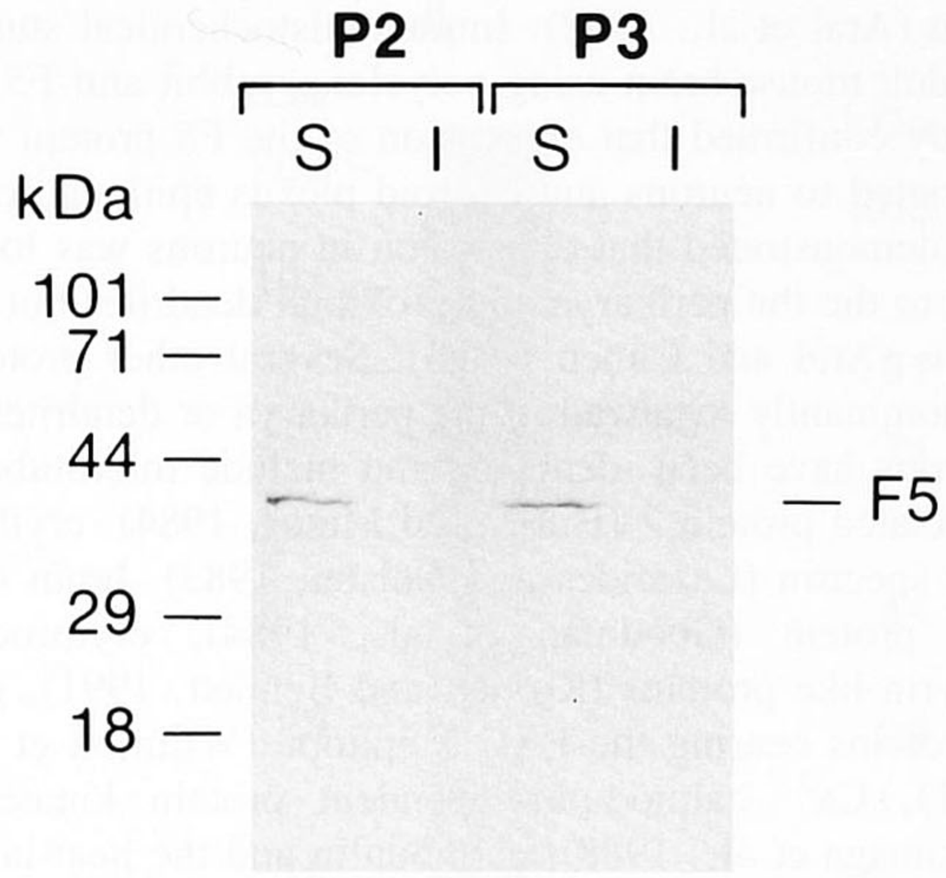

Fig. 5. Alkaline extraction of P2 and P3 fractions. Aliquots of P2 and P3 fractions were incubated in 0.1 M sodium carbonate, pH 11.5. After centrifugation, the soluble protein in the aqueous phase (S) and the insoluble pellet (I) were analyzed by SDS-PAGE and Western blotting with anti-F5 antibody. All of the F5 protein in the P2 and P3 fractions was soluble in sodium carbonate and was removed by alkaline extraction to the aqueous phase.

Very little protein is detected in the 10% and 30% sucrose steps. By Western blotting, β-tubulin and actin, which are found in both the membrane-associated and cytoplasmic components of the cytoskeleton (Willmott et al., 1991), were almost equally distributed among the 10/30% sucrose interface, 30/50% interface, and 50% sucrose step (Fig. 7). NF-M immunoreactivity, which is restricted to the cytoplasmic cytoskeleton (Willmott et al., 1991), was strong in the 50% sucrose step and 30/50% interface but minimal in the 10/30% interface. In contrast, F5 immunoreactivity was greatly enriched in the 10/30% fraction with a lower level in the 30/50% fraction. Very little was found in the 50% sucrose step fraction. Thus, a significant proportion of the F5 protein in neurons is associated with the cytoskeleton, predominantly with the membrane skeleton rather than the cytoplasmic cytoskeleton.

Association of F5 Protein With PSDs

Localization of F5 immunoreactivity in the detergent-insoluble material derived from the P2B synaptosomal subfraction and association of the F5 protein with the membrane cytoskeleton suggested that the F5 protein was a component of the PSD, a specialization of the neuronal membrane-associated cytoskeleton located under the postsynaptic membrane. PSDs were isolated by a standard method (Cohen et al., 1977). Western blotting with anti-F5 antibody demonstrated strong immunoreac-

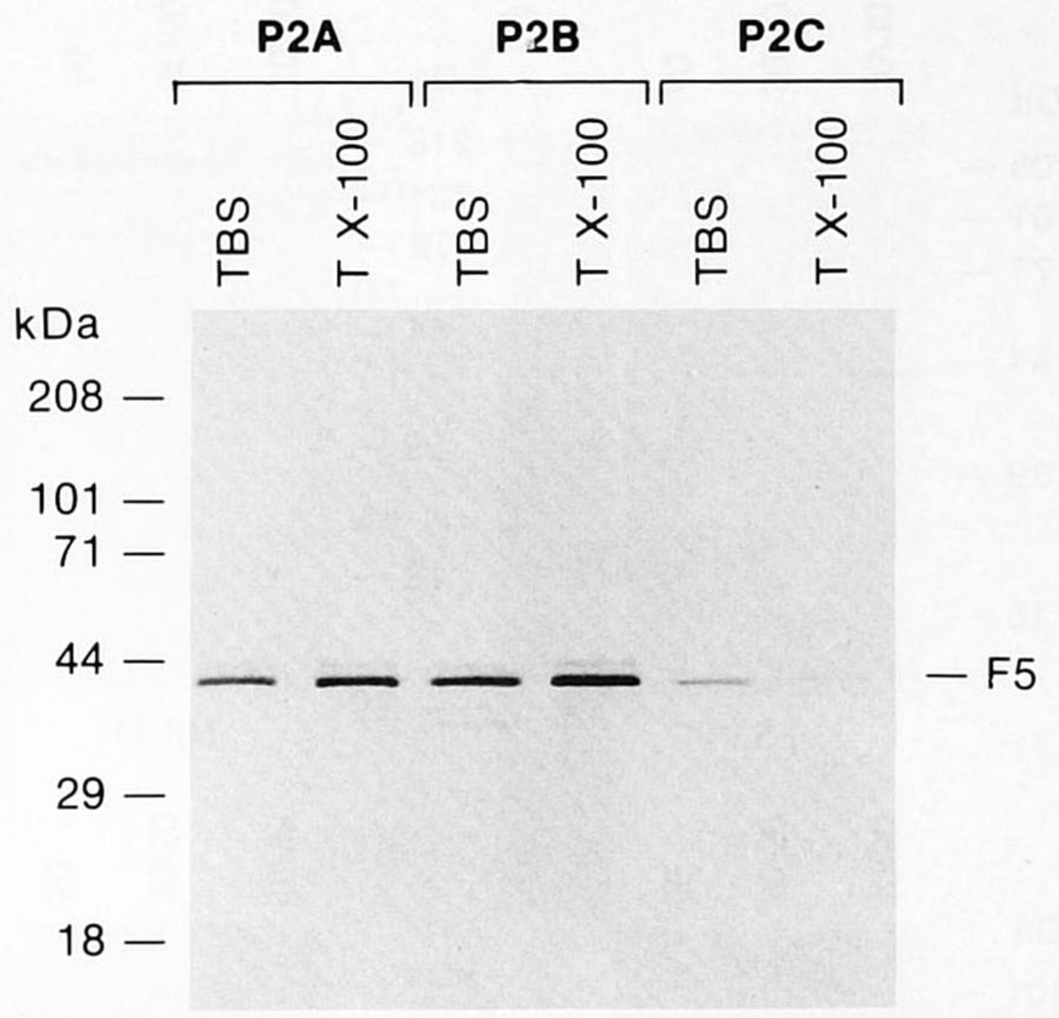

Fig. 6. Detergent extraction of P2 subfractions. Aliquots of the myelin (P2A), synaptosomal (P2B), and mitochondrial (P2C) subfractions containing 200 μg protein were extracted twice with 2% Triton X-100 (T X-100) at a high detergent to protein ratio of 100:1. Incubation of each subfraction in 50 mM TBS (TBS) served as a negative control. After centrifugation, insoluble pellets were analyzed by SDS-PAGE and Western blotting with anti-F5 antibody. Virtually none of the F5 protein in the P2A and P2B subfractions was soluble in detergent. In contrast, all but approximately 12% of the P2C-associated F5 protein was extracted by nonionic detergent.

tivity with an apparent molecular weight of 42 kDa (Fig. 8), confirming association of the F5 protein with the PSD. A Coomassie brilliant blue-stained gel of the PSD preparation showed the characteristic major PSD proteins with apparent molecular weights of 51 and 55 kDa (Flanagan et al., 1982), but did not demonstrate a band with apparent molecular weight corresponding to that of the F5 protein. Thus, the F5 protein does not appear to be a major component of PSD. Western blotting with digoxigenin-conjugated ConA showed two major glycoproteins with apparent molecular weights of 180 and 130 kDa and four minor bands of 245, 145, 110, and 80 kDa, typical of PSD (Gurd et al., 1982). No band corresponding to the F5 protein was seen, confirming previous studies (M. Arai, unpublished data) showing that the F5 protein in brain is not glycosylated.

DISCUSSION

F5 is a novel neuroimmune marker originally identified as an mRNA induced in T-lymphocytes in association with an interleukin-2-stimulated proliferative re-

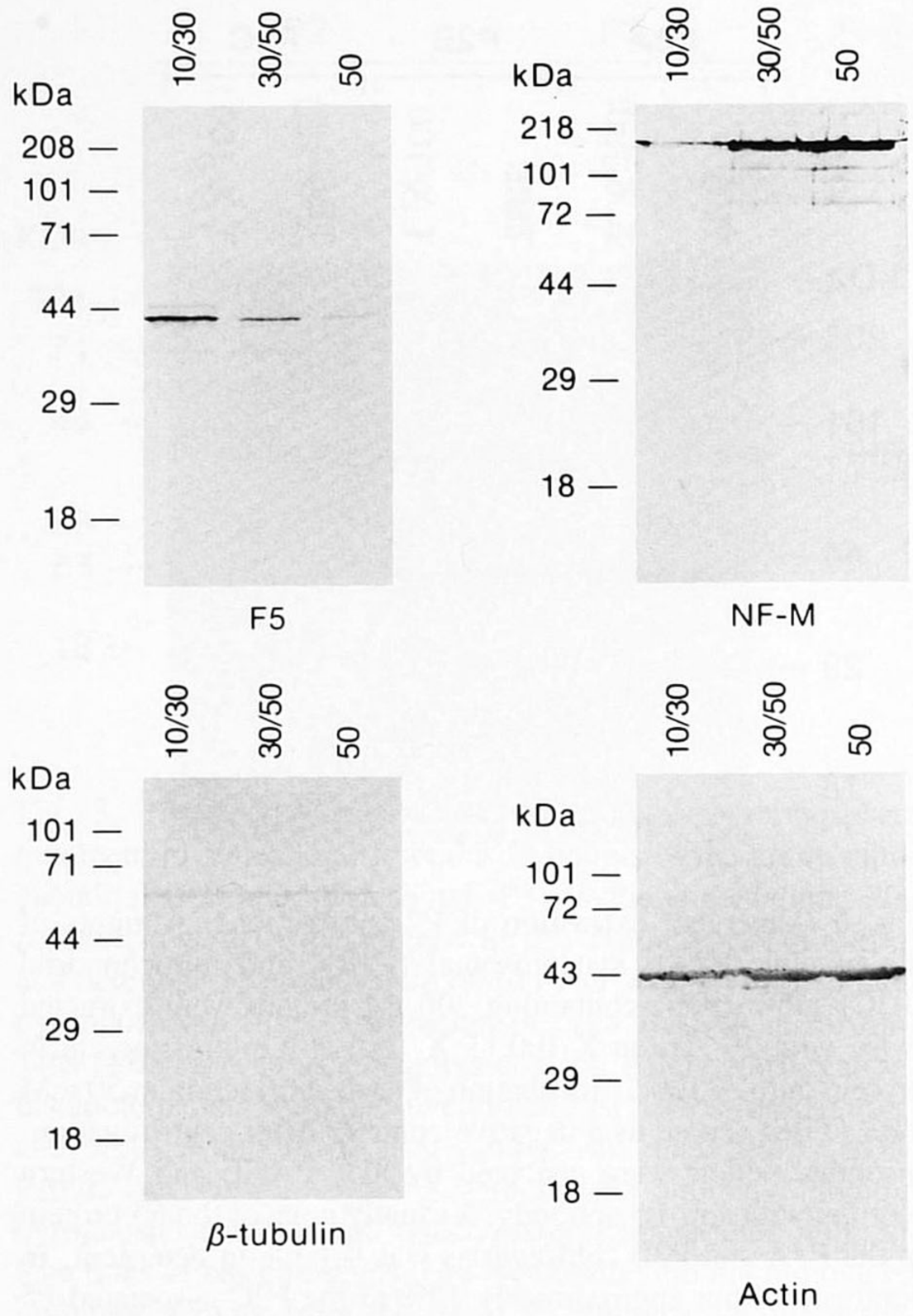

Fig. 7. Localization of the F5 protein in the membrane-associated cytoskeleton fraction. Triton X-100-insoluble material from adult mouse brain was fractionated by centrifugation on a discontinuous sucrose gradient. Aliquots of the 10/30% sucrose interface, 30/50% interface, and 50% sucrose step fractions containing 20 μg protein were analyzed by SDS-PAGE and Western blotting. The blots were stained for F5, NF-M, β-tubulin, and pan-actin. F5 immunoreactivity was detected at the highest level at the 10/30% interface, which contains membrane-associated cytoskeleton. It was present at a very low level in the 50% step, containing the cytoplasmic cytoskeleton, and at an intermediate level in the 30/50% interface, which contains a mixture of the two cytoskeletal components. NF-M immunoreactivity was found in the 50% step and at a lower level at the 30/50% interface. Both β-tubulin and pan-actin reactivity were found in all three fractions.

sponse (Sabath et al., 1990). F5 mRNA was found to have an interesting expression pattern, with expression restricted to proliferating T-lymphocytes and to the nervous system (Cohen et al., 1992) (J.A. Cohen, unpublished data). Within the nervous system, the F5 mRNA was expressed by mature neurons and choroid plexus epithelial cells, both of which are postmitotic in the adult brain (Arai et al., 1992). Immunohistochemical studies of adult mouse brain using polyclonal rabbit anti-F5 antibody confirmed that expression of the F5 protein was restricted to neurons and choroid plexus epithelial cells and demonstrated that expression in neurons was localized to the the perikarya and proximal dendrites but not axons (Arai and Cohen, 1993). Several other proteins predominantly localized in the perikarya or dendrites of neurons have been identified and include microtubule-associated protein 2 (Huber and Matus, 1984), erythrocyte spectrin (Lazarides and Nelson, 1983), brain 4.1-like protein (Goodman et al., 1984), erythrocyte ankyrin-like proteins (Kordeli and Bennett, 1991), glycoproteins bearing the PAC 1 epitope (Willmott et al., 1991), Ca^{2+}/calmodulin-dependent protein kinase II (Fukunaga et al., 1988), calmodulin and the heat-labile calmodulin-binding protein CaM-BP_{80} (Wood et al., 1980), the γ-subspecies of protein kinase C (Kose et al., 1990), and phosphotyrosine protein phosphatase activity (Yoshioka et al., 1991). Thus, the F5 protein represents an additional marker distinguishing dendrites from axons. The asymmetric intracellular distribution of these proteins suggests that they play a role in maintaining the morphological or functional polarity of neurons. The mRNAs for erythroid ankyrin and microtubule-associated protein 2 (Garner et al., 1988; Tucker et al., 1989; Peters et al., 1991) and polyribosomes containing their mRNAs (Steward and Falk, 1986) can be found in neuronal dendrites, suggesting that these dendrite-specific proteins are synthesized locally in the dendritic cytoplasm. In contrast, F5 mRNA is found exclusively in the neuronal perikarya (Arai et al., 1992). Thus, the intracellular transport mechanism for the F5 protein appears to be different from that for erythroid ankyrin and microtubule-associated protein 2.

The present studies were undertaken to define more precisely the subcellular localization of the F5 protein. The results of these studies were somewhat surprising. The deduced sequence of the F5 protein predicted a hydrophilic, basic protein without hydrophobic domains, leader sequence, or motifs characteristic of integral membrane or transmembrane proteins (Cohen et al., 1992). Recombinant F5 protein was freely soluble (Arai and Cohen, 1993). However, after subcellular fractionation essentially no F5 immunoreactivity was detected in the cytosol. Rather, the F5 immunoreactivity was restricted to the particulate fractions. Within P2, the crude mitochondrial fraction, F5 immunoreactivity was greatly enriched in the P2B synaptosomal subfraction, but not in the P2A myelin or P2C mitochondrial subfractions.

The particulate fractions contain both membrane and cytoskeletal components. The present studies suggested that the F5 protein was associated with both. The lack of effect of sodium pyrophosphate treatment made it

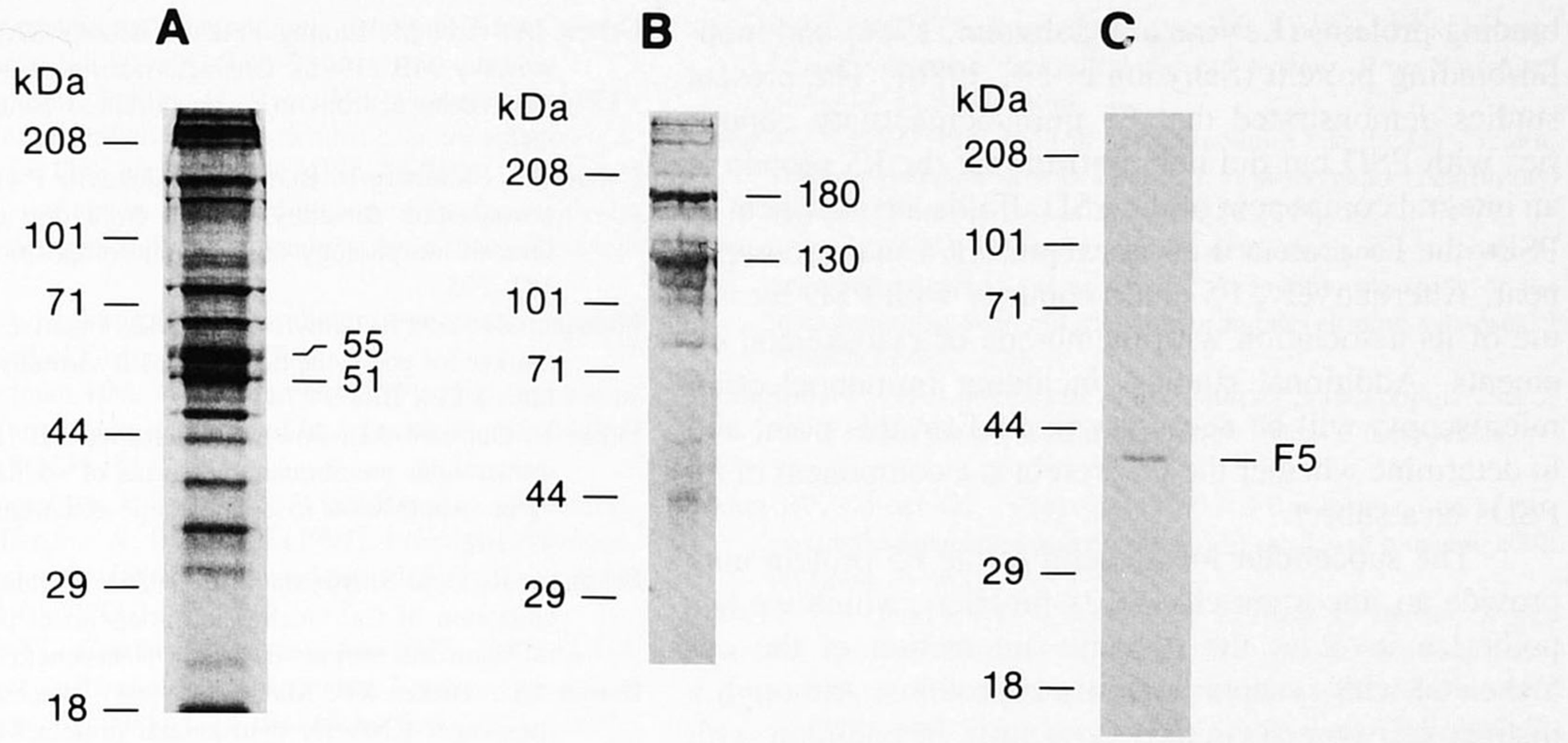

Fig. 8. F5 immunoreactivity within the PSD fraction. The PSD fraction was isolated from Triton X-100-insoluble material from adult mouse brain by discontinuous sucrose gradient centrifugation. **A:** Purified PSD material was analyzed by SDS-PAGE. The gel was stained with Coomassie brilliant blue, demonstrating the predominant 51- and 55-kDa bands plus a large number of additional bands. **B:** Isolated PSD material was analyzed by SDS-PAGE and then Western blotting. The blot was stained with digoxigenin-conjugated ConA and alkaline phosphatase-conjugated anti-digoxigenin antibody, demonstrating the characteristic 180- and 130-kDa glycoproteins. **C:** An aliquot of the PSD fraction containing 5 μg protein was analyzed by SDS-PAGE and Western blotting with anti-F5 antibody, demonstrating strong immunoreactivity.

unlikely that F5 immunoreactivity in the P2 and P3 fractions represented nonspecific binding to membrane components. The results of studies employing temperature-dependent phase separation with Triton X-114 and alkaline extraction with sodium carbonate demonstrated that the F5 protein was associated with but extrinsic to the membrane. These results also suggested that a covalent linkage via fatty acid acylation, polyisoprenylation, or glycosylphosphatidylinositol membrane anchoring was unlikely to be the mechanism by which the F5 protein binds to membrane.

There was a striking difference in regard to solubility of the F5 protein in nonionic detergent in the P3 microsomal fraction and the P2 mitochondrial fraction, particularly the P2A and P2B subfractions. Virtually all of the P3-associated F5 immunoreactivity was detergent-soluble. Most (approximately 80%) of the P2-associated F5 immunoreactivity also was detergent-soluble, probably representing the immunoreactivity found at low concentration in the P2C purified mitochondrial subfraction, which constitutes the largest component of the P2 fraction. However, a sizable proportion (approximately 20%) of the P2-associated immunoreactivity was detergent-insoluble, probably corresponding to the F5 protein found in the P2A myelin and P2B synaptosomal subfractions, of which virtually 100% was detergent-insoluble. Thus, the F5 protein found at low concentration in the P3 crude microsomal fraction and P2C purified mitochondria fraction appeared to be associated with membrane components. In contrast, the F5 protein in the P2B synaptosomal subfraction, where it was present at a high concentration, and the P2A subfraction appeared to be associated with cytoskeletal elements. Direct isolation of brain cytoskeleton confirmed this association. Furthermore, these studies showed that the F5 protein was found with the membrane-associated cytoskeleton rather than the cytoplasmic cytoskeleton.

PSDs are proteinaceous, electron-dense discs lying opposite the presynaptic terminal on the cytoplasmic side of the postsynaptic membrane of most chemical synapses in the central and peripheral nervous systems. A large number of studies suggest that PSDs are involved in maintaining synaptic structure by anchoring receptors and ion channels in the postsynaptic membrane (Siekevitz, 1985, 1991). The PSDs also have been postulated to play a critical role in synaptic transmission and synaptic plasticity. For example, both biochemical and morphological changes in the hippocampal PSD have been shown to occur in long-term potentiation, a model of learning, and kindling, a model of epilepsy (Siekevitz, 1985). PSDs represent unique specializations of the membrane-associated cytoskeleton and contain a variety of cytoskeletal proteins, such as actin (Blomberg et al., 1977; Matus et al., 1982), tubulin (Kelly and Cotman, 1978), and brain spectrin (Carlin et al., 1983), and cytoskeleton-associated proteins, such as brain spectrin-

binding proteins (LeVine and Sahyoun, 1986) and tubulin-binding protein (Sahyoun et al., 1986). The present studies demonstrated that F5 immunoreactivity copurifies with PSD but did not confirm that the F5 protein is an integral component of the PSD. If it is a component of PSD, the F5 protein does not represent a major component. Alternatively, F5 could copurify with PSD by virtue of its association with membrane or cytoskeletal elements. Additional studies, including immunoelectron microscopy, will be necessary to confirm this point and to determine whether the F5 protein is a component of all PSDs or a subset.

The subcellular localization of the F5 protein may provide an important clue to its function, which we hypothesize involves the dynamic interaction of the cytoskeletal with synaptic membrane proteins. Although a distinct cell type seemingly with little in common with neurons, T-lymphocytes also must maintain a multimeric receptor structure in the plasma membrane, namely the T-lymphocyte antigen-receptor complex. Thus, it will be of great interest to determine whether the F5 protein has an analogous subcellular localization in T-lymphocytes, i.e., an association with cytoskeletal and membrane elements.

ACKNOWLEDGMENTS

This work was supported by National Institutes of Health Award NS-08075 and Clinician-Investigator Development Award NS-01284 to J.A.C. and a long-term International Human Frontier Science Program postdoctoral fellowship to M.A.

REFERENCES

Amar-Costesec A, Wibo M, Thines-Sempoux D, Beaufay H, Berthet J (1974): Analytical study of microsomes and isolated subcellular membranes from rat liver. IV. Biochemical, physical, and morphological modifications of microsomal components induced by digitonin, EDTA, and pyrophosphate. J Cell Biol 62:717–745.

Arai M, Cohen JA (1993): Characterization of the neuroimmune protein F5: Localization to the dendrites and perikarya of mature neurons and the basal aspect of choroid plexus epithelial cells. J Neurosci Res 36:305–314.

Arai M, Prystowsky MB, Cohen JA (1992): Expression of the T-lymphocyte activation gene, F5, by mature neurons. J Neurosci Res 33:527–537.

Blomberg F, Cohen RS, Siekevitz P (1977): The structure of postsynaptic densities isolated from dog cerebral cortex. II. Characterization and arrangement of some of the major proteins within the structure. J Cell Biol 74:204–225.

Bordier C (1981): Phase separation of integral membrane proteins in Triton X-114 solution. J Biol Chem 256:1604–1607.

Carlin RK, Bartelt DC, Siekevitz P (1983): Identification of fodrin as a major calmodulin-binding protein in postsynaptic density preparations. J Cell Biol 96:443–448.

Cohen JA, Arai M, Luning Prak E, Brooks SA, Young LH, Prystowsky MB (1992): Characterization of a novel mRNA expressed by neurons in mature brain. J Neurosci Res 31:273–284.

Cohen RS, Blomberg F, Berzins K, Siekevitz P (1977): Structure of postsynaptic densities isolated from dog cerebral cortex. I. Overall morphology and protein composition. J Cell Biol 74: 181–203.

Flanagan SD, Yost B, Crawford G (1982): Putative 51,000-Mr protein marker for postsynaptic densities is virtually absent in cerebellum. J Cell Biol 94:743–748.

Fujiki Y, Hubbard AL, Fowler S, Lazarow PB (1982): Isolation of intracellular membranes by means of sodium carbonate treatment: Application to endoplasmic reticulum. J Cell Biol 93: 97–102.

Fukunaga K, Goto S, Miyamoto E (1988): Immunohistochemical localization of Ca^{2+}/calmodulin-dependent protein kinase II in rat brain and various tissues. J Neurochem 51:1070–1078.

Garner CC, Tucker RP, Matus A (1988): Selective localization of messenger RNA for cytoskeletal protein MAP2 in dendrites. Nature 336:674–677.

Goodman SR, Casoria LA, Coleman DB, Zagon IS (1984): Identification and location of brain protein 4.1. Science 224:1443–1446.

Gray EG, Whittaker VP (1962): The isolation of nerve endings from brain: An electron-microscopic study of cell fragments derived by homogenization and centrifugation. J Anat 96:79–88.

Gurd JW, Jones LR, Mahler HR, Moore WJ (1974): Isolation and partial characterization of rat brain synaptic plasma membranes. J Neurochem 22:281–290.

Gurd JW, Gordon-Weeks P, Evans WH (1982): Biochemical and morphological comparison of postsynaptic densities prepared from rat, hamster, and monkey brains by phase partitioning. J Neurochem 39:1117–1124.

Huber G, Matus A (1984): Differences in the cellular distributions of two microtubule-associated proteins, MAP1 and MAP2, in rat brain. J Neurosci 4:151–160.

Kelly PT, Cotman CW (1978): Synaptic proteins. Characterization of tubulin and actin and identification of a distinct postsynaptic density polypeptide. J Cell Biol 79:173–183.

Kordeli E, Bennett V (1991): Distinct ankyrin isoforms at neuron cell bodies and nodes of Ranvier resolved using erythrocyte ankyrin-deficient mice. J Cell Biol 114:1243–1259.

Kose A, Ito A, Saito N, Tanaka C (1990): Electron microscopic localization of γ- and βII-subspecies of protein kinase C in rat hippocampus. Brain Res 518:209–217.

Krueger BK, Forn J, Greengard P (1977): Depolarization-induced phosphorylation of specific proteins, mediated by calcium ion influx, in rat brain synaptosomes. J Biol Chem 252:2764–2773.

Lazarides E, Nelson WJ (1983): Erythrocyte and brain forms of spectrin in cerebellum: Distinct membrane-cytoskeletal domains in neurons. Science 220:1295–1296.

Lee VM-Y, Carden MJ, Schlaepfer WW, Trojanowski JQ (1987): Monoclonal antibodies distinguish several differentially phosphorylated states of the two largest rat neurofilament subunits (NF-H and NF-M) and demonstrate their existence in the normal nervous system of adult rats. J Neurosci 7:3474–3488.

LeVine HI, Sahyoun NE (1986): Involvement of fodrin-binding proteins in the structure of the neuronal postsynaptic density and regulation by phosphorylation. Biochem Biophys Res Commun 138:59–65.

Maher PA, Singer SJ (1985): Anomalous interaction of the acetylcho-

line receptor protein with the nonionic detergent Triton X-114. Proc Natl Acad Sci USA 82:958–962.

Matus A, Ackermann M, Pehling G, Byers HR, Fujiwara K (1982): High actin concentrations in brain dendritic spines and postsynaptic densities. Proc Natl Acad Sci USA 79:7590–7594.

Moss DJ (1983): Cytoskeleton-associated glycoproteins from chicken sympathetic neurons and chicken embryo brain. Eur J Biochem 135:291–297.

O'Farrell PH (1975): High resolution two-dimensional electrophoresis of protein. J Biol Chem 250:4007–4021.

O'Farrell PZ, Goodman HM, O'Farrell PH (1977): High resolution two-dimensional electrophoresis of basic as well as acidic proteins. Cell 12:1133–1142.

Peters LL, Birkenmeier CS, Bronson RT, White RA, Lux SE, Otto E, Bennett V, Higgins A, Barker JE (1991): Purkinje cell degeneration associated with erythroid ankyrin deficiency in *nb/nb* mice. J Cell Biol 114:1233–1241.

Sabath DE, Podolin PL, Comber PG, Prystowsky MB (1990): cDNA cloning and characterization of interleukin 2-induced genes in a cloned T helper lymphocyte. J Biol Chem 265:12671–12678.

Sahyoun N, LeVine HI, McDonald OB, Cuatrecasas P (1986): Specific postsynaptic density proteins bind tubulin and calmodulin-dependent protein kinase type II. J Biol Chem 261:12339–12344.

Scheele GA, Palade GE, Tartakoff AM (1978): Cell fractionation studies on the guinea pig pancreas. Redistribution of exocrine proteins during tissue homogenization. J Cell Biol 78:110–130.

Siekevitz P (1985): The postsynaptic density: A possible role in long-lasting effects in the central nervous system. Proc Natl Acad Sci USA 82:3494–3498.

Siekevitz P (1991): Possible role for calmodulin and the Ca^{2+}/calmodulin-dependent protein kinase II in postsynaptic neurotransmission. Proc Natl Acad Sci USA 88:5374–5378.

Steward O, Falk PM (1986): Protein-synthetic machinery at postsynaptic sites during synaptogenesis: A quantitative study of the association between polyribosomes and developing synapses. J Neurosci 6:412–423.

Thompson RJ (1973): Studies of RNA synthesis in two populations of nuclei from the mammalian cerebral cortex. J Neurochem 21: 19–40.

Tucker RP, Garner CC, Matus A (1989): In situ localization of microtubule-associated protein mRNA in the developing and adult rat brain. Neuron 2:1245–1256.

Willmott TG, Selkirk CP, Hawkes RB, Philippe E, Gordon-Weeks PR, Beesley PW (1991): PAC 1: An epitope associated with two novel glycoprotein components of isolated postsynaptic densities and a novel cytoskeleton-associated polypeptide. Neuroscience 44:627–641.

Wood JG, Wallace RW, Whitaker JN, Cheung WY (1980): Immunocytochemical localization of calmodulin and a heat-labile calmodulin-binding protein ($CaM\text{-}BP_{80}$) in basal ganglia of mouse brain. J Cell Biol 84:66–76.

Yoshioka T, Tanaka O, Otani H, Shinohara H (1991): Histochemically demonstrable phosphotyrosine protein phosphatase in the rat hippocampal formation. Brain Res 555:177–179.